Energy Reports 8 (2022) 13793–13813

Contents lists available at ScienceDirect

Energy Reports

journal homepage: www.elsevier.com/locate/egyr

Review article

An overview of water electrolysis technologies for green hydrogen production

S. Shiva Kumar [a], Hankwon Lim [a,b,c,*]

[a] Carbon Neutrality Demonstration and Research Center, Ulsan National Institute of Science and Technology, 50 UNIST-gil, Eonyang-up, Ulju-gun, Ulsan 44919, Republic of Korea
[b] Graduate School of Carbon Neutrality, Ulsan National Institute of Science and Technology, 50 UNIST-gil, Eonyang-up, Ulju-gun, Ulsan 44919, Republic of Korea
[c] School of Energy and Chemical Engineering, Ulsan National Institute of Science and Technology, 50 UNIST-gil, Eonyang-up, Ulju-gun, Ulsan 44919, Republic of Korea

ARTICLE INFO

Article history:
Received 21 July 2022
Received in revised form 21 September 2022
Accepted 6 October 2022
Available online xxxx

Keywords:
Green hydrogen production
Alkaline water electrolysis
Anion exchange membrane water electrolysis
Proton exchange membrane water electrolysis
Solid oxide water electrolysis

ABSTRACT

Decarbonizing the planet is one of the major goals that countries around the world have set for 2050 to mitigate the effects of climate change. To achieve these goals, green hydrogen that can be produced from the electrolysis of water is an important key solution to tackle global decarbonization. Consequently, in recent years there is an increase in interest towards green hydrogen production through the electrolysis process for large-scale implementation of renewable energy-based power plants and other industrial, and transportation applications. The main objective of this study was to provide a comprehensive review of various green hydrogen production technologies especially on water electrolysis. In this review, various water electrolysis technologies and their techno-commercial prospects including hydrogen production cost, along with recent developments in electrode materials, and their challenges were summarized. Further some of the most successful results also were described. Moreover this review aims to identify the gaps in water electrolysis research and development towards the techno-commercial perspective. In addition, some of the commercial electrolyzer performances and their limitations also were described along with possible solutions for cost-effective hydrogen production Finally, we outlined our ideas, and possible solutions for driving cost-effective green hydrogen production for commercial applications. This information will provide future research directions and a road map for the development/implementation of commercially viable green hydrogen projects.

Contents

* Corresponding author at: Carbon Neutrality Demonstration and Research Center, Ulsan National Institute of Science and Technology, 50 UNIST-gil, Eonyang-up, Ulju-gun, Ulsan 44919, Republic of Korea.
E-mail addresses: sampangishiva@gmail.com (S. Shiva Kumar), hklim@unist.ac.kr (H. Lim).

https://doi.org/10.1016/j.egyr.2022.10.127

1. Introduction

Global energy demand and consumption are always on the rise due to an increase in population and standards of living, apart from the industrial growth of developing countries (Ibrahim, 2012; Mostafa et al., 2019). Inductively the global primary energy supply was 14,410 MTOE in 2019 (IEA, 2019a). According to the International energy agency's prediction, the global energy demand will be increased by 50% in 2030 (EIA, 2016). To date, more than 95% of this huge energy demand is fulfilled by using fossil fuels, however, the use of fossil fuels releases a high concentration of greenhouse gas emissions consequently increasing the global warming and environmental pollution (Sazal, 2020; Lee et al., 2018). Therefore, the rapid development of alternative green energy technologies is essential to meet global energy demands and sustainable development. In this context, the 'Paris Agreement' was framed and approved by 196 parties at the 21st conference of the parties (COP 21) in 2015, which aims to respond to the global warming actively by preventing a global temperature rise below 1.5 °C (Jacquet and Jamieson, 2016). In addition, many countries have focused on introducing environmentally friendly energy policies for a sustainable environment and decarbonization. For example, South Korea announced the 2nd Climate Change Response Master Plan in 2019 to reduce greenhouse gas emissions from 709.1 million tons in 2017 to 536 million tons by 2030 for a sustainable and low-carbon green society (Lee et al., 2020). Thus, globally various research institutions/organizations have moved towards the development of innovative technologies that can utilize renewable sources for generating green energy and fuels. Hydrogen is one such promising environmentally friendly renewable energy carrier and it is the most abundant element in the universe (Immanuel and Dmitri, 2018; Pinsky et al., 2020; Dawood et al., 2020). The hydrogen atom is composed of one proton and one electron, making it the lightest element in the universe, and having unique properties like high energy density (120 MJ/kg) and lower volumetric energy density (8 MJ/L). However, it is not readily available directly on the earth, it is available in chemically combined forms of water, fossil fuels, and biomass. Hence the main challenge is to separate hydrogen from the naturally occurring compounds efficiently and economically.

2. Hydrogen production

Hydrogen can be produced from various sources of raw materials including renewable and non-renewable sources which are around 87 million tons/year (Dawood et al., 2020; Milani et al., 2020). However, as of 2020, most of the hydrogen (95%) was produced from non-renewable fossil fuels especially steam reforming of natural gas, emitting 830 million tons/year of CO_2 and the rest of the hydrogen was produced from renewable resources including water electrolysis (Mosca et al., 2020; IEA, 2019b). The major hydrogen production methods and their applications are as shown in Fig. 1.

Hydrogen is classified into different color shades i.e., blue, gray, brown, black, and green respectively based on their hydrogen production technology, energy source, and environmental impact (Noussan et al., 2021; Ajanovic et al., 2022), as shown in Table 1. The blue hydrogen is produced from the steam reforming of natural gas. During this process, natural gas is split into hydrogen (H_2) and carbon dioxide (CO_2), the produced CO_2 is captured (85%–95%) and stored underground using industrial carbon capture and storage techniques and some of the generated CO_2 cannot be captured. In addition, long-term impacts of storage are uncertain, and leakage can still negatively affect the environment and climate (Hermesmann and Muller, 2022; Navas-Anguita et al., 2021). The gray hydrogen is produced from non-renewable fossil fuels such as natural gas or coal by steam reforming/auto-thermal reforming process, this process is similar to the blue hydrogen process, but the produced CO_2 is not being captured, it is directly released into the atmosphere (Nikolaidis and Poullikkas, 2017). Brown hydrogen is most abundant in use today, which is produced from hydrocarbon-rich feedstock (brown coal or methane) via the gasification process. But as a result, every tone of brown hydrogen releases 10–12 tons of CO_2 into the atmosphere. The black hydrogen is produced from coal gasification, during this coal gasification process syngas are produced from the gasifier and the hydrogen can be separated from the other gases using absorbers or special membranes and the remaining gases can be released into the atmosphere (IRENA, 2020a; IEA, 2019b). Green hydrogen is produced from renewable water and electricity by electrolysis process, in this process water is split into hydrogen (H_2) and oxygen (O_2) under the influence of electricity with zero carbon emissions (Carmo et al., 2013).

In the transition towards global decarbonization, nowadays renewable-powered green hydrogen generation is one way that is increasingly being considered as a means of reducing greenhouse gas emissions and environmental pollution (Yue et al., 2021; Burton et al., 2021). Hence, there is an increasing interest to make the production and utilization of this green hydrogen more scalable and versatile process. Water electrolysis is a key technology for splitting water into hydrogen and oxygen by using renewable energy (solar, wind) (Ibrahim, 2012; Burton et al., 2021). Solar and wind energies are prepared and well suitable renewable power sources for hydrogen production through water electrolysis due to their widespread power distribution (Wang et al., 2014). The combination of renewable energy with water electrolysis is particularly more advantageous because surplus electrical energy can be stored chemically in the form of hydrogen to balance the discrepancy between energy demand and production (Brauns and Thomas, 2020). Further, the produced hydrogen and oxygen can be directly used for the transportation and industrial sector as primary energy sources. Hydrogen is not only a primary energy source it is an energy carrier that can be directly used in fuel cell vehicles and the industrial sector. Moreover, hydrogen can also

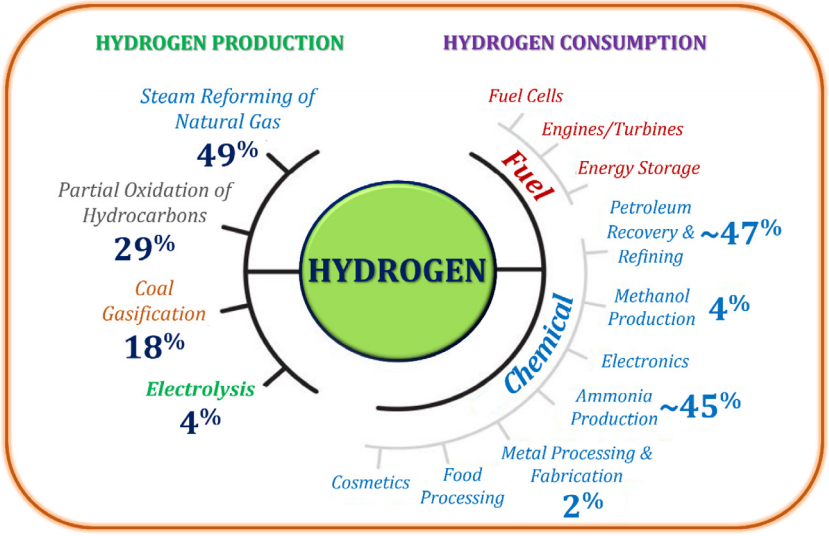

Fig. 1. Major hydrogen production methods and applications. . (For interpretation of the references to color in this figure legend, the reader is referred to the web version of this article.)

Table 1
Hydrogen color shades and their Technology, cost, and CO_2 emissions.

Hydrogen Color	Technology	Source	Products	Cost ($ kg/H_2)	CO_2 emissions
Brown Hydrogen	Gasification	Brown coal (Lignite)	$H_2 + CO_2$	1.2–2.1	High
Black Hydrogen	Gasification	Black coal (Bituminous)	$H_2 + CO_2$	1.2–2.1	High
Grey Hydrogen	Reforming	Natural gas	$H_2 + CO_2$ (Released)	1–2.1	Medium
Blue Hydrogen	Reforming + carbon capture	Natural gas	$H_2 + CO_2$ (Captured 85-95%)	1.5–2.9	Low
Green Hydrogen	Electrolysis	Water	$H_2 + O_2$	3.6–5.8	Minimal

be used as a feedstock in chemical and petrochemical industries to produce ammonia and synthetic fuels (Jovan and Dolanc, 2020; Shiva Kumar and Himabindu, 2019a; Shiva Kumar et al., 2019b). Apart from that, another advantage of hydrogen as an energy carrier is the increased efficiency of hydrogen storage systems when compared to batteries.

2.1. Significant role of green hydrogen in energy transition

Green hydrogen is widely viewed as a promising fuel for future sustainable development and energy transition due to fact that green hydrogen can be produced from water and renewable energy sources through the electrolysis process, in this process there are no greenhouse gas emissions. Therefore, green hydrogen is increasingly being promoted to address climate change issues and meet the global net-zero challenges. Moreover, global demand for green hydrogen and its applications is expected to increase exponentially over the next decade. Fortunately, globally some projects are already underway to produce green hydrogen from renewable energy sources like wind and solar (IEA, 2021).

3. Water electrolysis

Water electrolysis is one such electrochemical water splitting technique for green hydrogen production with the help of electricity, which is emission-free technology. The basic reaction of water electrolysis is as follows in Eq. (1).

$$1\ H_2O + \text{Electricity}\ (237.2\ \text{kJ mol}^{-1}) + \text{Heat}\ (48.6\ \text{kJ mol}^{-1}) \longrightarrow H_2 + {}^1/_2\,O_2 \quad (1)$$

The above reaction (Eq. (1)) requires 1.23 V theoretical thermodynamic cell voltage to split the water into hydrogen and oxygen at room temperature. However, experimentally the required cell voltage for efficient water splitting is 1.48 V. The additional voltage is required to overcome the kinetics and ohmic resistance of the electrolyte and cell components of the electrolyzer (Shiva Kumar and Himabindu, 2020; Lee et al., 2021b; Lim et al., 2021).

Past two centuries, water electrolysis is a well-known technology for green hydrogen production. However, globally only 4% of hydrogen (65 million tons) can be produced from water electrolysis due to economic issues, with most of this hydrogen being produced as a by-product from the Chlor-alkali industry (Yu et al., 2018; Hall et al., 2020; Yodwong et al., 2020). The largest electrolysis plant (135 MW/30,000 N m^3/h) has been deployed for the fertilizer industry (Bertuccioli et al., 2014a,b). Since the 18th century, water electrolysis technologies are being continuously developed and used in industrial applications, during this journey different trends have affected its development, with this split into roughly five generations. Each generation of water electrolysis and their challenges, technological breakthroughs, and significance are shown in Fig. 2.

During these developments, four types of water electrolysis technologies were introduced based on their electrolyte, operating conditions, and their ionic agents (OH^-, H^+, O^{2-}), such as (i) Alkaline water electrolysis (ii) AEM water electrolysis

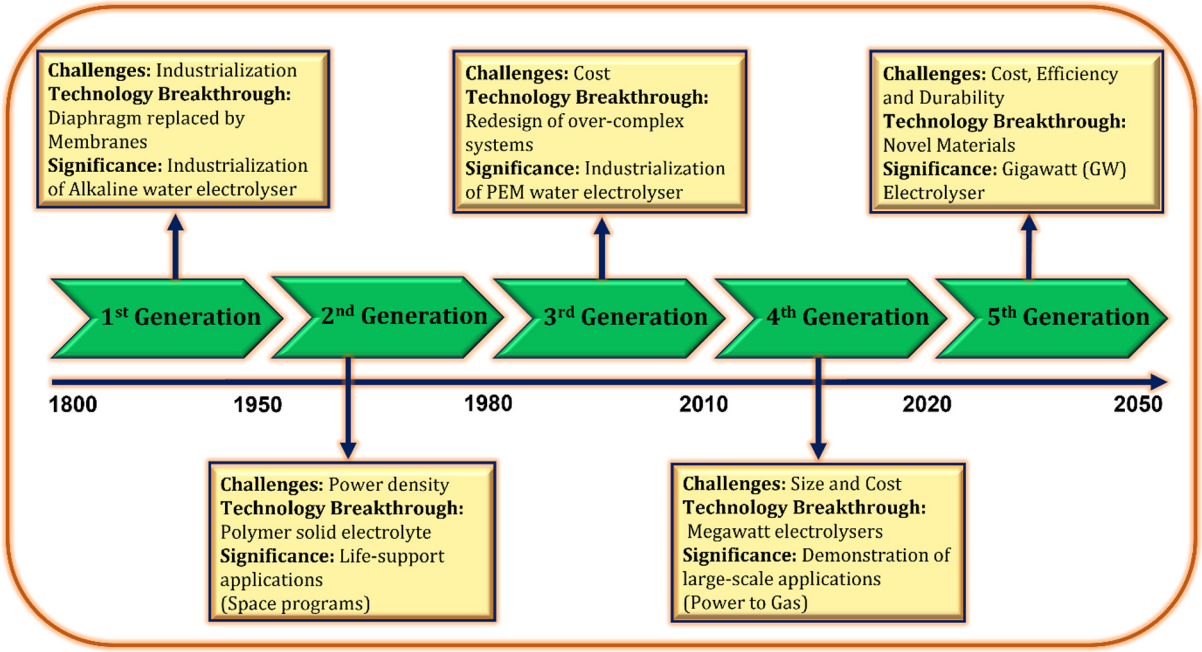

Fig. 2. Generations of water electrolysis development (IRENA, 2020b).

(iii) PEM water electrolysis and (iv) Solid oxide water electrolysis. However, the operating principles are the same for all the cases (Shiva Kumar and Himabindu, 2019a). The four types of water electrolysis technologies and their characteristics along with advantages, disadvantages were described in the following subsections and Tables 2 & 3.

3.1. Alkaline water electrolysis

Alkaline water electrolysis is well established mature technology for industrial hydrogen production up to the multi-megawatt range in commercial applications across the globe (Kuckshinrichs et al., 2017). The alkaline water electrolysis phenomenon was first introduced by Troostwijk and Diemann in the year 1789. After several developments in the year of 1939, the first industrial large-scale alkaline water electrolyzer plant with the capacity of 10,000 N m^3 H_2h^{-1} went into operation (Diogo et al., 2013). In later early 19th century, more than 400 industrial alkaline electrolyzer units were successfully installed and operated for industrial applications (Grigoriev et al., 2020). However, the alkaline water electrolyzer operates at lower temperatures (30–80 °C) with a concentrated alkaline solution (5M KOH/NaOH). Moreover, in alkaline water electrolyzer nickel (Ni) coated stainless steel electrodes and asbestos/ZrO_2-based diaphragms are used as a separator (Shiva Kumar et al., 2018a,b,c,d, 2017). The ionic charge carrier is hydroxyl ion (OH^-) with KOH/NaOH and water permeating through the porous structure of the diaphragm to provide the functionality of the electrochemical reaction (Shiva Kumar et al., 2017; Lee et al., 2021a). The alkaline water electrolysis is a favorable system design for large-scale applications. Today, the investment cost of alkaline water electrolysis is USD 500–1000/kW, and the lifetime of the system is 90,000 h (Bertuccioli et al., 2014a,b; Schmidt et al., 2017). However, the major challenge associated with alkaline water electrolysis is limited current densities (0.1–0.5 A/cm^2) due to moderate OH^- mobility, and usage of corrosive (KOH) electrolytes (IRENA, 2020a). Due to the high sensitivity of the KOH electrolyte to ambient CO_2 and the subsequent salt formation of K_2CO_3, the resulting decrease in the number of hydroxyl ions and ionic conductivity. In addition, the salt of K_2CO_3 close the pores of the anode gas diffusion layer which subsequently decreases the ion transferability through the diaphragm and consequent reduction of hydrogen production. Apart from that, the alkaline water electrolysis produces low purity (99.9%) of gasses (Hydrogen and Oxygen) due to the existing diaphragm does not completely prevent the crossover of the gases from one half-cell to the other.

3.1.1. Working principle of alkaline water electrolysis

Alkaline water electrolysis is an electrochemical water splitting techniques in the presence of electricity. The electrochemical water splitting consists of two individual half-cell reactions such as hydrogen evolution reaction (HER) at the cathode and oxygen evolution reaction (OER) at the anode. During the alkaline electrolysis process, initially at the cathode side two moles of alkaline solution are reduced to produce one mole of hydrogen (H_2) and two moles of hydroxyl ions (OH^-), the produced H_2 can be eliminated from the cathodic surface and the remaining hydroxyl ions (OH^-) are transferred under the influence of electric circuit between anode and cathode through the porous separator to the anode side. At the anode, the hydroxyl ions (OH^-) are discharged to produce the ½ molecule of oxygen (O_2) and one molecule of water (H_2O), as shown in Fig. 3.

3.1.2. Cell components of alkaline water electrolysis

The major alkaline water electrolysis cell components are diaphragms/separators, current collectors (gas diffusion layer), separator plates (bipolar plates), and end plates respectively. In general, Asbestos/Zirfon/Nickel coated perforated stainless-steel diaphragms are used as separators in alkaline water electrolysis (David et al., 2019; Shiva Kumar et al., 2017). The nickel mesh/foam is used as gas diffusion layers and stainless steel/nickel-coated stainless steel separator plates are used as bipolar and end plates respectively.

Table 2
Technical characteristics of typical water electrolysis technologies (IRENA, 2020b).

	Alkaline	AEM	PEM	Solid Oxide
Anode reaction	$2OH^- \rightarrow H_2O + \frac{1}{2} O_2 + 2e^-$	$2OH^- \rightarrow H_2O + \frac{1}{2} O_2 + 2e^-$	$H_2O \rightarrow 2H^+ + \frac{1}{2} O_2 + 2e^-$	$O^{2-} \rightarrow \frac{1}{2} O_2 + 2e^-$
Cathode Reaction	$2 H_2O + 2e^- \rightarrow H_2 + 2OH^-$	$2 H_2O + 2e^- \rightarrow H_2 + 2OH^-$	$2H^+ + 2e^- \rightarrow H_2$	$H_2O + 2e^- \rightarrow H_2 + O^{2-}$
Overall cell	$H_2O \rightarrow H_2 + \frac{1}{2} O_2$	$H_2O \rightarrow H_2 + \frac{1}{2} O_2$	$2H_2O \rightarrow H_2 + \frac{1}{2} O_2$	$H_2O \rightarrow H_2 + \frac{1}{2} O_2$
Electrolyte	KOH/NaOH (5M)	DVB polymer support with 1 M KOH/NaOH	Solid polymer electrolyte (PFSA)	Yttria stabilized Zirconia (YSZ)
Separator	Asbestos/Zirfon/Ni	Fumatech,	Nafion®	Solid electrolyte YSZ
Electrode/Catalyst (Hydrogen side)	Nickel coated perforated stainless steel	Nickel	Iridium oxide	Ni/YSZ
Electrode/Catalyst (Oxygen side)	Nickel coated perforated stainless steel	Nickel or NiFeCo alloys	Platinum carbon	Perovskites (LSCF, LSM) (La,Sr,Co,FE) (La,Sr,Mn)
Gas Diffusion layer	Nickel mesh	Nickel foam/carbon cloth	Titanium mesh/carbon cloth	Nickel mesh/foam
Bipolar Plates	Stainless steel/Nickel coated stainless steel	Stainless steel/Nickel coated stainless steel	Platinum/Gold-coated Titanium or Titanium	Cobalt coated stainless steel
Nominal current density	0.2–0.8 A/cm^2	0.2–2 A/cm^2	1–2 A/cm^2	0.3–1 A/cm^2
Voltage range (limits)	1.4–3 V	1.4–2.0 V	1.4–2.5 V	1.0–1.5 V
Operating temperature	70–90 °C	40–60 °C	50–80 °C	700–850 °C
Cell pressure	<30 bar	<35 bar	<70 bar	1 bar
H2 purity	99.5–99.9998%	99.9–99.9999%	99.9–99.9999%	99.9%
Efficiency	50%–78%	57%–59%	50%–83%	89% (laboratory)
Lifetime (stack)	60 000 h	>30 000 h	50 000–80 000 h	20 000 h
Development status	Mature	R & D	Commercialized	R & D
Electrode area	10 000–30 000 cm^2	<300 cm^2	1500 cm^2	200 cm^2
Capital costs (stack) minimum 1 MW	USD 270/kW	Unknown	USD 400/kW	>USD 2000/kW
Capital costs (stack) minimum 10 MW	USD 500–1000/kW	Unknown	USD 700–1400/kW	Unknown

Table 3
Advantages and disadvantages of typical water electrolysis technologies.

Electrolysis technology	Advantages	Disadvantages
Alkaline water electrolysis	• Well established Technology • Commercialized for industrial applications • Noble metal-free electrocatalysts • Relatively low cost • Long-term stability	• Limited current densities • Crossover of the gasses • High concentrated (5M KOH) liquid electrolyte
AEM water electrolysis	• Noble metal-free electrocatalysts • Low concentrated (1M KOH) liquid electrolyte.	• Limited stability • Under development
PEM water electrolysis	• Commercialized technology • Operates higher current densities • High purity of the gases • Compact system design • Quick response	• Cost of the cell components • Noble metal electrocatalysts • Acidic electrolyte
Solid oxide water electrolysis	• High working temperature • High efficiency	• Limited stability • Under development

3.1.3. Research and development of alkaline water electrolysis

Alkaline water electrolysis is a mature and well-established technology up to the multi-megawatt scale and globally number of manufacturers are successfully deployed and used for industrial applications (IRENA, 2020b; IEA, 2021), some of the commercial alkaline water electrolyzers and their manufacturers are listed in Table 4. However, some improvements are still needed in this technology such as increase in the current density and reduce the crossover of the gasses. To achieve these challenges, new electrode materials and separators need to be developed. Moreover, an alkaline water electrolyzer can be integrated with renewable energy (solar, wind) sources which can be more beneficial for reducing the capital cost. In this direction, some of the research institutes/organizations are still actively working on increasing the efficiency and reducing hydrogen production cost. For example, Liu et al. (2020) reported heterojunction hybrid structures of MoS_2@$Ni_{0.96}S$ as a low-cost and noble metal-free bifunctional electrocatalysts for OER and HER in alkaline media. The developed MoS_2@$Ni_{0.96}S$-1 electrocatalyst exhibited a significantly lower overpotential of 104 mV at 10 mA cm^{-2} towards the HER and OER overpotential of 182 mV at 10 mA cm^{-2} with the highest HER and OER activity. Additionally, achieved a lower cell voltage of 1.86 V for the overall water splitting and demonstrated superior stability during the continuous operation of 15 h. This improvement is mainly due to strong integration between ultrathin MoS_2 nanosheets with non-stoichiometric $Ni_{0.96}S$ nanocrystals, exposure of more active sites, and presence of abundant heterojunction interfaces within MoS_2@$Ni_{0.96}S$-1h. Qazi et al.

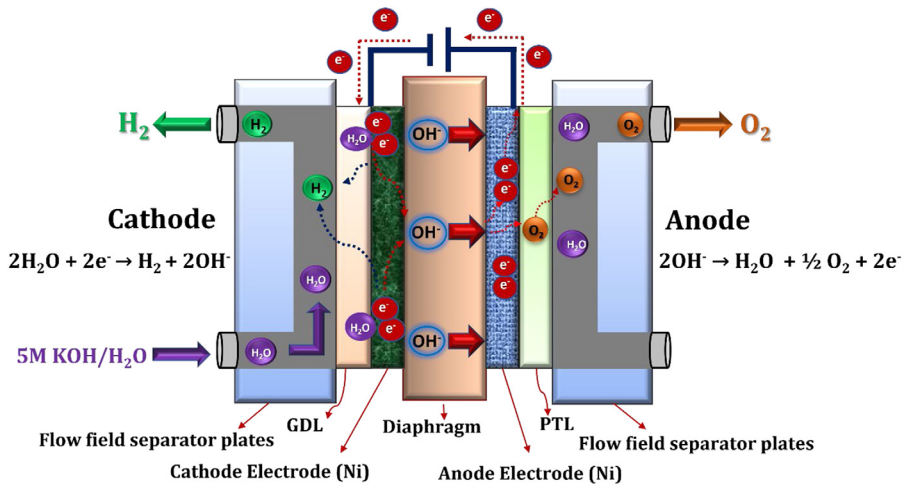

Fig. 3. Schematic illustration of alkaline water electrolysis working principle.

(2021) developed an efficient bifunctional nano heterostructure electrocatalyst of NiCo-$NiCoO_2$@Cu_2O@CF for overall water splitting and studied their performance in 1M KOH solution. As prepared NiCo-$NiCoO_2$@Cu_2O@CF electrocatalyst has shown improved electrochemical performance towards the HER and OER in alkaline media with a lower overpotential of 133 and 327 mV to achieve a current density of 10 mA cm^2 with a small Tafel slope of 119 and 118 mV dec^{-1} for HER and OER respectively. In addition, experimentally studied their performance through single-cell electrolysis process using NiCo-$NiCoO_2$@Cu_2O@CF as a bifunctional electrocatalyst for both HER and OER. The results showed better electrochemical performance than the other non-noble metal electrocatalysts, the attained cell voltage of 1.69 V to reach the current density $\geq$10 mA cm^{-2}. Further, the developed electrocatalyst was stable during the continuous electrolysis process of 12 h in a strong alkaline solution due to the robust mechanical adhesion between NiCo-$NiCoO_2$ nanoparticles. The better performance was achieved by the small size of NiCo-$NiCoO_2$ nano heterostructures uniformly distributed on the oxidized surface of copper foam enabling them to maximum utilization active sites during the electrochemical reactions. Xu et al. (2022) developed a highly efficient bifunctional electrocatalyst of 2D metal–organic framework (MOF)-derived NiCoP nanoflakes ($NiCo_{(nf)}$-P) for overall water splitting in alkaline media. The developed electrocatalyst performance were studied by three-electrode cell assembly with linear sweep voltammetry (LSV) method at the potential cycling rate of 2 mV s^{-1} in a 1M KOH electrolyte solution. The developed $NiCo_{(nf)}$-P was shown better electrocatalytic activity with a lower onset potential of 37 mV and 1.435 V than commercial 5% Pt/C (43 mV) and IrO_2 (1.504 V) at the current density of 100 mV cm^{-2} towards the HER and OER. In addition, $NiCo_{(nf)}$-P was shown lower overpotential of 119 mV and 315 mV than commercial 5% Pt/C (291 mV) and IrO_2 (400) to achieve the current density of 100 mV cm^{-2} towards the HER and OER. The Tafel slope also potentially lower for $NiCo_{(nf)}$-P (112 mV dec^{-1}) and 66 mV dec^{-1} than commercial 5% Pt/C (164 mV dec^{-1}) and IrO_2 (88 mV dec^{-1}), which indicates the rapid charge transfer across the electrocatalytic interfaces of as developed $NiCo_{(nf)}$-P. Further, the developed $NiCo_{(nf)}$-P electrocatalyst stability studies were carried out at different current densities of 100, 500, and 1000 mA cm^{-2} towards the HER and OER using chronopotentiometric (V-t) measurements. The, attained results show the stable electrochemical performance during the 30 h of continuous operation, as shown in Fig. 4. Moreover, the developed $NiCo_{(nf)}$-P electrocatalyst HER and OER performance also were studied in alkaline electrolyzer, it shows the excellent electrocatalytic activity with a lower cell voltage of 1.94 V at the operating current density of 1 A cm^{-2}.

Further, Jin et al. (2021) have synthesized N-doped carbon supported Ni-Mo-O/Ni_4Mo nanointerface electrocatalyst (Ni-Mo-O/Ni_4Mo@NC) by electrodeposition–calcination–electrodeposition techniques and studied their electrocatalytic activity towards the hydrogen evolution reaction in alkaline solution (1M KOH). The synthesized Ni-Mo-O/Ni_4Mo@NC electrocatalyst has shown a higher electrocatalytic activity with a lower overpotential of 61 mV at a geometric current density of 10 mA cm^{-2}, which is 50% lower than that of Ni-Mo-O (120 mV) due to the introduction of N-doped carbon layers. Also, studies in neutral conditions (1M PBS solution) Ni-Mo-O/Ni_4Mo@NC shows an overpotential of $<$ 60 mV, which is lower than that of Ni-Mo-O ($\sim$100 mV). The Tafel slope of Ni-Mo-O/Ni_4Mo@NC is determined to be 99 mV dec^{-1}, which is relatively lower than that of Ni-Mo-O (135 mV dec^{-1}). Lv et al. (2021) introduced multi-heterostructure interfaces and 3D porous structures of Co_2P/N@$Ti_3C_2T_x$@NF as an efficient HER electrocatalyst for alkaline media. Initially, CPN@TC with multi-heterostructure interfaces were fabricated on the surface of MXene ($Ti_3C_2T_x$)-modified NF by a two-step electrodeposition method and subsequent nitriding process. The prepared Co_2P/N@$Ti_3C_2T_x$@NF electrocatalyst performance was studied in 1M KOH solution, the results exhibited an outstanding HER performance with an overpotential of only 15 mV at 10 mA cm^{-2} and a small Tafel slope of 30 mV dec^{-1}, as shown in Fig. 5. In addition, shown superior stability during the 3000 cycles of CV tests and only 20 mV shifting can be at the current density of 100 mA cm^{-2}. In addition, water dissociation (ΔG_{*H_2O}) and hydrogen adsorption (ΔG_{*H}) energies were calculated by DFT (density functional theory) for different materials. According to the DFT calculations, the prepared CPN@TC has strongest binding energy of -0.822 eV, which is favorable for the HER reactions. Also, the prepared CPN@TC possesses an H* adsorption energy with the closest value to zero, which is generally considered to be the best electrocatalyst.

3.2. Anion exchange membrane (AEM) water electrolysis

AEM water electrolysis is a developing technology for green hydrogen production. Over the past few years, many research organizations/institutions are actively working in the development of AEMWE due to its low cost and high performance compared to the other conventional electrolysis technologies. The first journal publication on AEMWE was by We and Scott in 2011 latter many researchers are contributing to the development

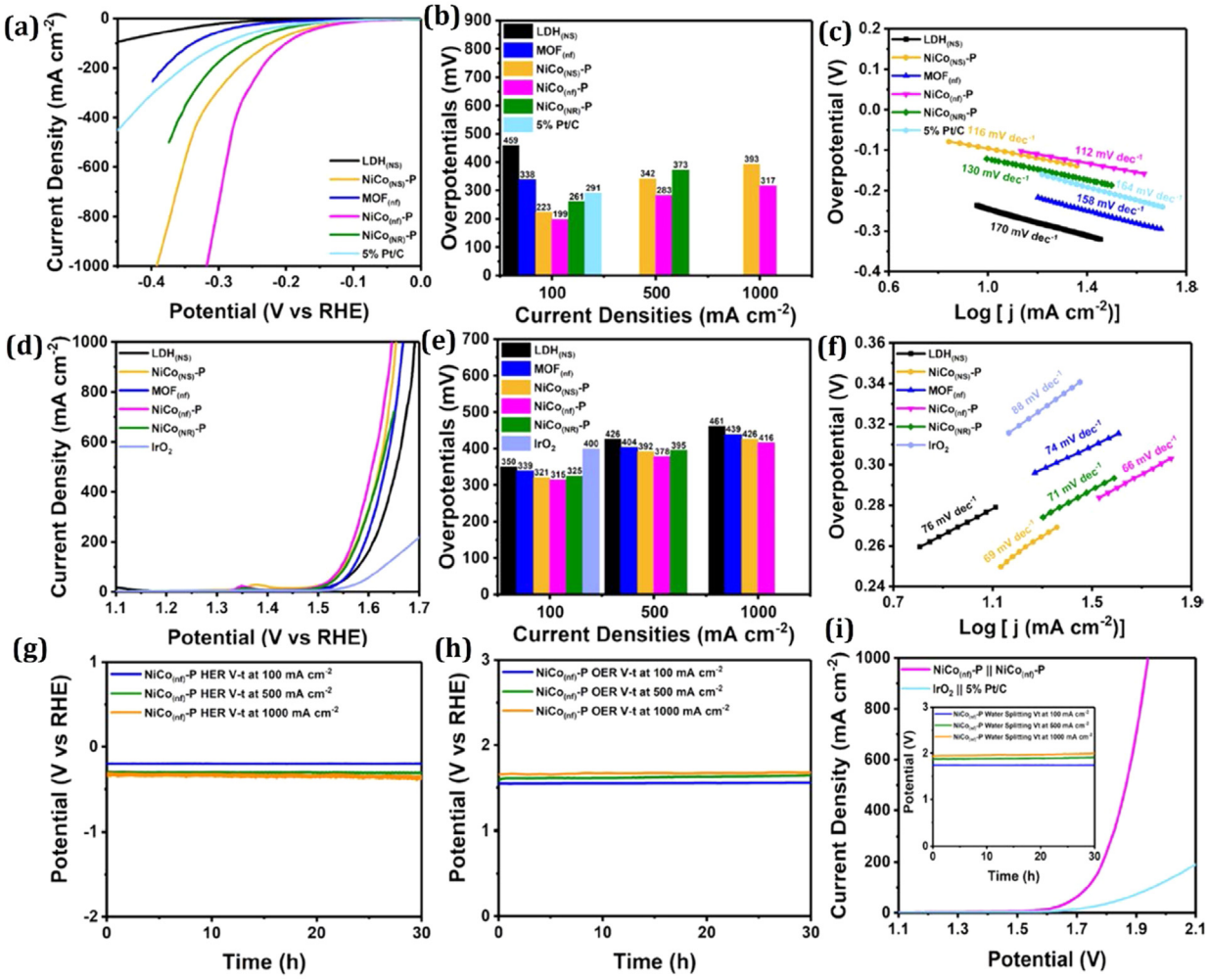

Fig. 4. Electrocatalytic activity of as synthesized electrocatalysts $LDH_{(NS)}$, $NiCo_{(NS)}$-P, $MOF_{(nf)}$, $NiCo_{(nf)}$-P, $NiCo_{(NR)}$-P, and commercial 5% Pt/C and IrO_2. (a) HER LSV curves, (b) HER overpotentials at different current densities of 100, 500, and 1000 mA cm^{-2} and (c) HER Tafel slopes. (d) OER LSV curves, (e) OER overpotentials at different current densities of 100, 500, and 1000 mA cm^{-2} (f) OER Tafel slopes (g, h) $NiCo_{(nf)}$-P electrocatalyst HER and OER stability studies (V-t curves) at different current densities of 100, 500, and 1000 mA cm^{-2} (i) LSV curves of NiCo(nf)-P and NiCo(nf)-P; Commercial IrO_2 and 5% Pt/C for overall water splitting. The inset is the V-t curves of $NiCo_{(nf)}$-P at current densities of 100, 500, and 1000 mA cm^{-2} towards overall water splitting (Xu et al., 2022).

of AEMWE (Wang et al., 2020a,b). The AEM water electrolysis technology is similar to conventional alkaline water electrolysis (Miller et al., 2020). However, the main difference between alkaline and AEM water electrolysis is the replacement of the conventional diaphragms (asbestos) with an anion exchange membrane (quaternary ammonium ion exchange membranes) in alkaline water electrolysis. AEM water electrolysis offers several advantages such as cost-effective transition metal catalysts being used instead of noble metal catalysts, distilled water/low concentrated alkaline solution (1M KOH) can be used as electrolyte instead of high concentrated (5 KOH solution) (Henkensmeier et al., 2021). Despite the significant advantages, AEMWE still required further investigations/improvements towards the MEA stability and cell efficiency which are more essential for large-scale or commercial applications. As of now, the reported stability is 2000 h with Sustain ion and 1000 h for Fumatech (A 201 and FAA3-50), and >35,000 h for Enapter multicore AEM electrolyzer (Pavel et al., 2014; Carbone et al., 2020; Enapter, Germany).

3.2.1. Working principle of AEM water electrolysis

AEM water electrolysis is one of the electrochemical water splitting techniques with the help of an anion exchange membrane and electricity. The electrochemical reaction consists of two half-cell reactions they are hydrogen evolution reaction (HER) and oxygen evolution reaction (OER). Initially, at the cathode side, the water molecule is reduced to generate hydrogen (H_2) and hydroxyl ions (OH^-) by the addition of two electrons. The hydrogen is released from the surface of cathode and the hydroxyl ions (OH^-) are diffused through the ion exchange membrane to the anode side by the positive attraction of the anode, while the electrons are transported through the external circuit to the anode. At the anode side, the hydroxyl ions recombine as a water molecules and oxygen by losing electrons. The produced oxygen is released from the anode. The basic principle and half-cell reactions of AEM water electrolysis as shown in Fig. 6.

3.2.2. Cell components of AEM water electrolysis

Generally, AEM water electrolysis cell components are membrane (separator), electrode materials current collectors (gas diffusion layer), separator plates (bipolar plates), and end plates respectively. Typical anion exchange membranes are quaternary ammonium ion exchange membranes i.e., Sustanion®, Fumasep, Fumatech respectively. Commonly used anode and cathode electrode materials are transition metal based electrocatalysts especially Nickel and NiFeCo alloy materials respectively. The nickel foam/porous nickel mesh and carbon cloth are used as anode and cathode gas diffusion layers. Stainless steel and nickel-coated

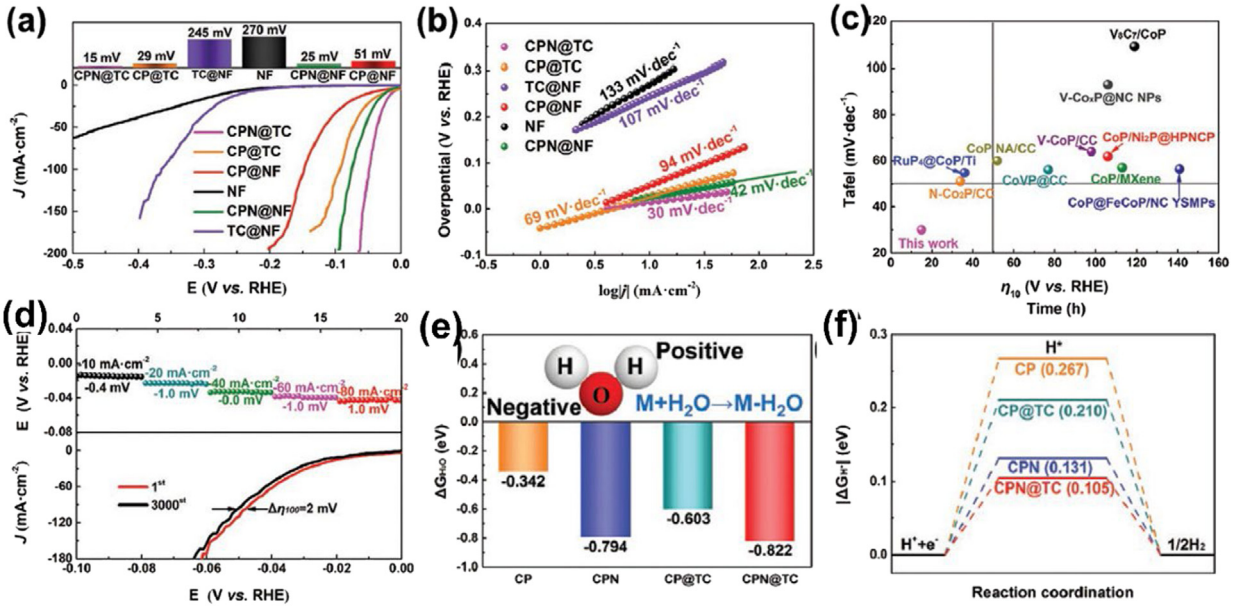

Fig. 5. (a) HER Polarization curves of CPN@TC, CP@TC, CP@NF, NF, CPN@NF and TC@NF (b) Tafel plots (c) comparison of CPN@TC with reported electrocatalysts (d) Long-term chronopotentiometry results of CPN@TC at different current densities (−10, −20, −40, −60, −80 mA cm^{-2}) and durability polarization curves for CPN@TC before and after 3000 cycles (e) Calculated H_2O adsorption energy. (f) H* adsorption energy (Lv et al., 2021).

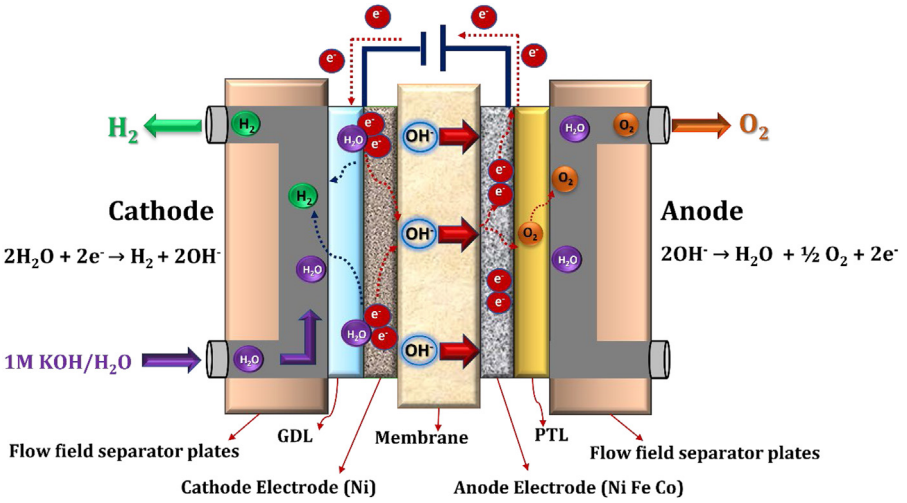

Fig. 6. Schematic view of AEM water electrolysis working principle.

stainless steel separator plates are used as bipolar and end plates respectively (Pushkareva et al., 2020).

3.2.3. Research and development of AEM water electrolysis

AEM water electrolysis technology is under the developmental stage up to the kW scale. Globally, several research organizations/institutions are actively working on the development of AEM water electrolyzers, some of the AEM water electrolyzer manufacturers/developers are listed in Table 4. However, several innovations/improvements are still needed to scale up this technology for commercial applications. The major challenges are limited stability (at present 35,000 h and targeted stability of 1,00,000 h) and high hydrogen production cost, present hydrogen production cost is USD 1279 kW/H_2 (2020), and the targeted cost reduction of USD $\leq$ 300 kW/H_2 (2050) (Ionomr, 2020). To achieve these targets, the existing challenges need to be addressed economically to commercialize for market applications. In this direction, Thangavel et al. (2021) developed a 3D oxygen evolution electrode via electrochemical integration of amorphous NiFeOOH on activated carbon fiber paper (CFP) by single-step co-electrodeposition techniques and their performance in 1M KOH solution. The developed 3D-a-NiFeOOH/N-CFP electrode has shown a better electrochemical performance with an overpotential of only 170 mV at a current density of 10 mA cm^{-2} and a smaller Tafel slope of 39 mV dec^{-1} and outstanding stability in 1M KOH solution, as shown in Fig. 7. This enhancement is due to the unique 3D structures with increased active sites and the enhanced electrical conductivity that helps enhance the OER kinetics and mass transport properties. In addition, Fe-doping plays a key role in enhanced OER activity of 3D-a-NiFeOOH/N-CFP. Additionally, the developed 3D-a-NiFeOOH/N-CFP electrode OER activity was studied in a single-cell alkaline AEM water electrolyzer with ultra-pure water and compared with commercial IrO_2 electrodes under similar experimental conditions. Impressively, the developed 3D-a-NiFeOOH/N-CFP electrode exhibits superior electrochemical performance to commercial IrO_2 electrodes, the attained cell voltage of 1.88 V than commercial IrO_2 2.08 V at

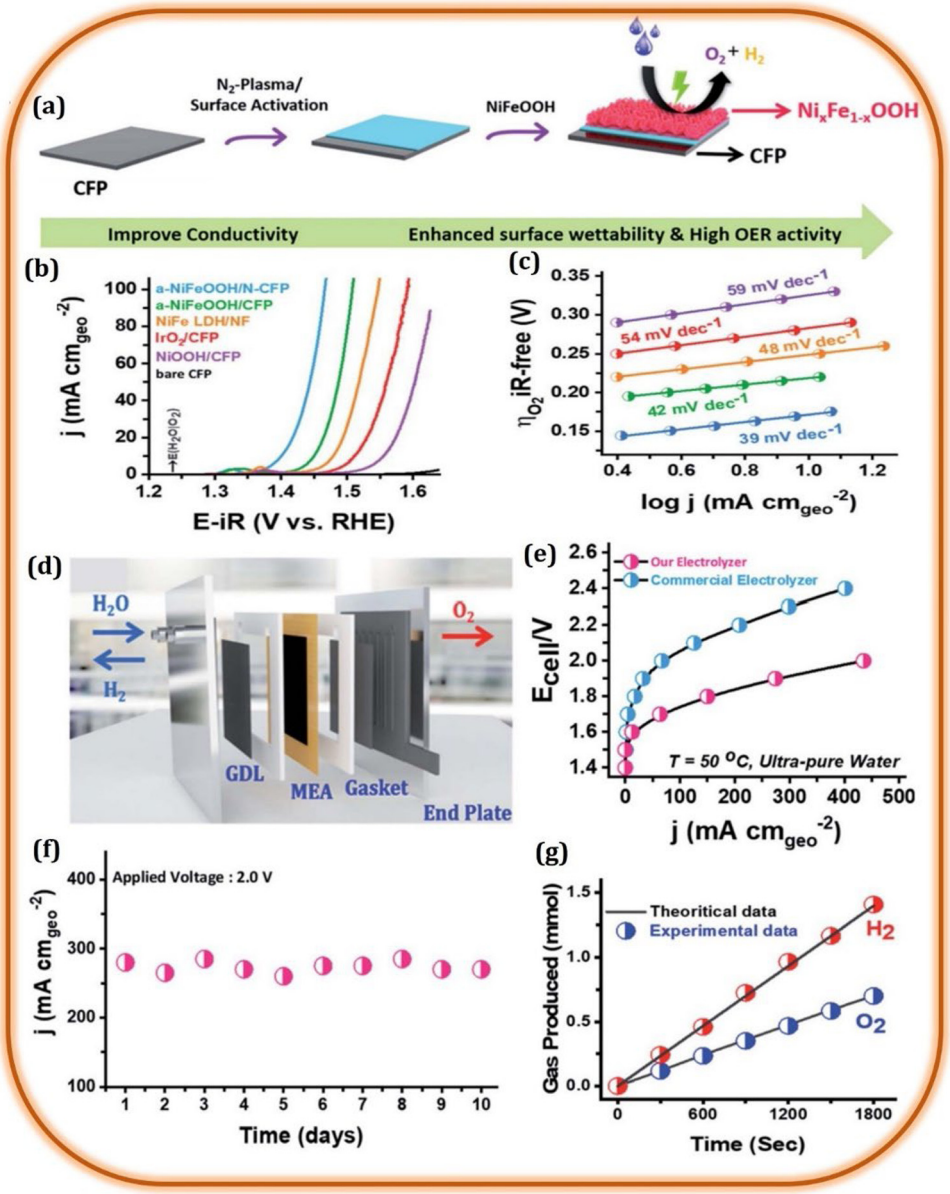

Fig. 7. (a) Schematic representation of 3D-a-NiFeOOH/N-CFP synthesis procedure. (b) LSV curves of various synthesized electrodes in 1 M KOH solution at a scan rate of 1 mV s^{-1}. (c) OER Tafel plots (d) Schematic view of the alkaline AEM water electrolyzer cell. (e) Current–Voltage polarization curves of the alkaline AEM water electrolysis fabricated with 3D-a-NiFeOOH/N-CFP and commercial IrO_2-based anodes at 50 °C. (e) Long-term stability of a-NiFeOOH/N-CFP electrode in electrolyzer with a constant cell voltage of 2.0 V for 10 days (g) Experimental and theoretical hydrogen yields (Faradaic efficiency) calculated through water displacement system (Thangavel et al., 2021).

an operating current density of 1 A/cm^2 with ∼80% energy efficiency. Furthermore, long-term stability is studied at constant voltage of 20.V for 240 h continuously where the prepared 3D-a-NiFeOOH/N-CFP electrode exhibited stability retention of 95.6% with ultra-low degradation rate of 0.15 mA h^{-1} and the Faradaic efficiency of 98.5%.

Guo et al. (2021) reported the facile and rapid synthesis of Cu-Co-P on carbon paper (CP) substrate using the electrodeposition technique. Initially, Co-P/CP deposition conditions are optimized and studied for HER in alkaline solution, the attained results showed acceptable electrocatalytic activity with an overpotential of 72 mV at a current density of 10 mA cm^{-2}. Further modified the surface properties including the electronic structure and increased the active sites of Co-P by incorporating Cu for enhancing the electrochemical performance. The modified Cu-Co-P1200/CP exhibited superior performance with an ultra-low overpotential of 59 mV at a current density of 10 mA cm^{-2} and a smaller Tafel slope of 38 mV dec^{-1}, as shown in Fig. 8. Moreover, the synthesized Cu-Co-P1200/CP performance studied towards the hydrogen evolution reaction as a cathode electrode in a single cell AEM water electrolyzer with an anode material of commercial IrO_2/CP, the achieved cell voltage of 1.9 V at an operating current density of 0.70 A cm^{-2} with good stability, which is slightly lower than that of noble metal-based electrodes of Pt/C/CP@IrO_2/CP. But this performance is superior to those in literature for non-noble metal-based electrodes.

Further, Jang et al. (2020a,b) synthesized a noble metal-free nanosized $Cu_{0.5}Co_{2.5}O_2$ anode electrocatalyst via co-precipitation technique by adjusting the pH for AEM water electrolysis and studied their performance in alkaline solution as well as water electrolyzer.

The synthesized $Cu_{0.5}Co_{2.5}O_2$ electrode exhibited improved electrochemical performance with an overpotential of 285 mV

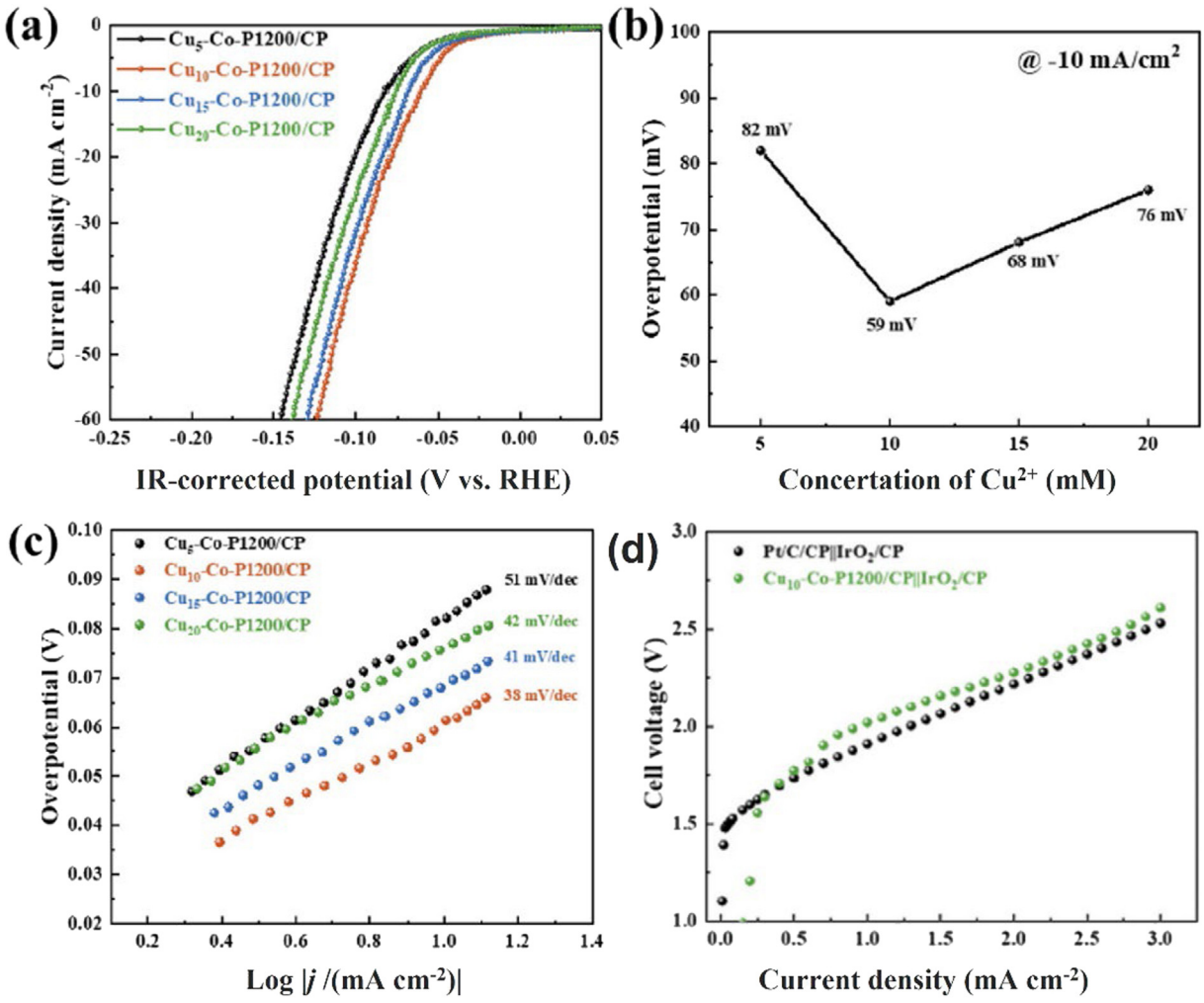

Fig. 8. (a) HER polarization curves of Cu-Co-P1200/CP electrodes with different concentrations of Cu^{2+} in 1M KOH solution with scan rate of 5 mV s^{-1} (b) (e) effect of Cu^{2+} concentration on overpotential at constant current density of 10 mA/cm^2 (c) Tafel slopes (d) Current–Voltage polarization cures of single cell AEM water electrolyzer with IrO_2/CP as anode coupled with as synthesized Cu_{10}-Co-P1200/CP electrode as cathode and compared with the commercial Pt/C/CP (Guo et al., 2021).

at 10 mA cm^{-2} in 1M KOH solution. Further, the developed $Cu_{0.5}Co_{2.5}O_2$ electrocatalyst performance was studied in a single-cell with the active area of 4.9 cm^2 AEM water electrolyzer as an anode and commercial Pt/C used as a cathode, the archived current density of 1.3 A cm^{-2} at 1.8 V at 45 °C with 1M KOH solution. Furthermore, durability studies were carried out for 100 h continuously at a constant current density of 400 mA cm^{-2} it maintained 80% energy efficiency during 100 h operation. In addition, demonstrated excellent stability at constant current density of 10 mA cm^{-2} for 2000 h. Chen et al. (2021) developed poly (fluorenyl-co-aryl piperidinium) (PFAP)-based anion exchange materials i.e., membrane electrolyte and binder with high ionic conductivity and durability under alkaline media. The developed electrolyte with platinum group metal (PGM) catalysts (IrO_2 and Pt/C) achieved a new record cell performance of 7.68 A/cm^2 at 2 V with 1M KOH and PGM-free materials (Ni-Fe) displayed an outstanding current density of 1.62 A cm^{-2} at 2.0 V. Additionally, PGM and PGM-free materials displayed excellent durability of more than 1000 h of operation at the constant current density of 0.5 A cm^{-2} at 60 °C without any voltage degradation.

3.3. PEM water electrolysis

To overcome the drawbacks of alkaline water electrolysis, the 1st PEM water electrolysis phenomenon was idealized by Grubbs and developed by General Electric Co. in the year of 1966 (Shiva Kumar and Himabindu, 2019a). However, PEM water electrolysis technology is similar to the PEM fuel cell technology, here the sulfonated polymer membrane can be used as an electrolyte. The ionic charge carrier is H^+ and DI water permeating through the proton-conducting membrane it provides the functionality of the electrochemical reaction. Typically, PEM water electrolysis operates at lower temperatures (30–80 °C) with higher current densities (1–2 A/cm^2) and produces high purity (99.999%) of gases (Hydrogen and Oxygen) (Shiva Kumar and Himabindu, 2019a). Because the kinetics of hydrogen evolution reaction in PEM water electrolysis is faster than alkaline water electrolysis due to the highly active area of the metal surface of Pt electrodes and lower pH of the electrolyte. In addition, PEM water electrolysis is safer than alkaline water electrolysis due to the absence of caustic electrolytes and smaller footprint. Therefore, globally several water electrolyzer manufacturers (listed in Table 4) are developed large-scale (up to MW) PEM water electrolyzers for industrial and transportation applications. The reported stability of PEMWE is 60,000 h with negligible loss of performance and the targeted stability is 1,00,000 h (Schmidt et al., 2017; Wei et al., 2019). However, the major challenges associated with the PEM water electrolysis are high cost of the components i.e., electrode materials, current collectors, and bipolar plates respectively.

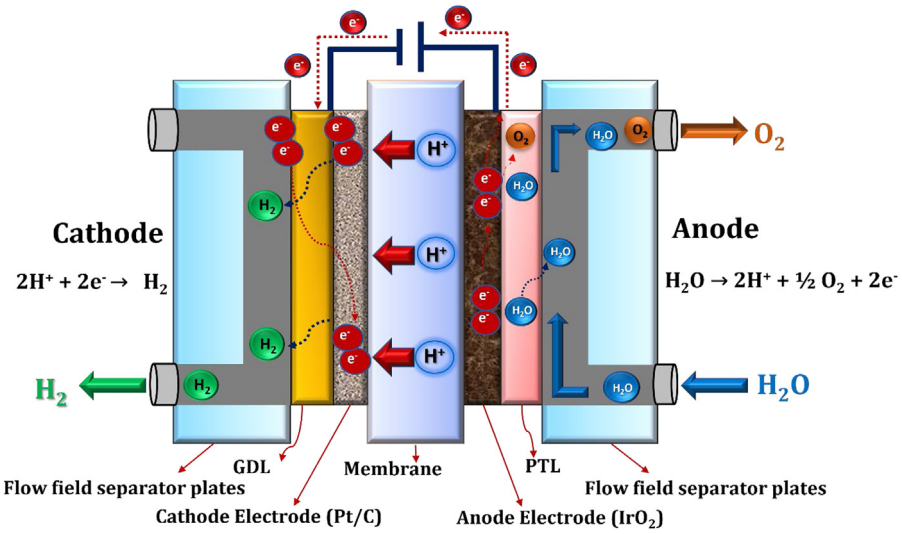

Fig. 9. Schematic view of PEM water electrolysis working principle.

3.3.1. Working principle of pem water electrolysis

During the PEM water electrolysis process, water is electrochemically split into hydrogen and oxygen. In this process, initially at the anode side water molecule is decomposed to generate oxygen (O_2) and protons (H^+), and electrons (e^-). The generated oxygen eliminated from the anodic surface and the remaining protons are traveled through the proton-conducting membrane to the cathode side and the electrons are traveled through the external circuit to the cathode side. At the cathode side, the protons and electrons recombined to produce H_2 gas. The basic principle of PEM water electrolysis is shown in Fig. 9.

3.3.2. Cell components of PEM water electrolysis

The PEM water electrolysis cell major components are membrane electrode assembly (consist of membrane and anode, cathode electrode materials), Gas diffusion layer, separator plates (bipolar plates), and end plates respectively (Shiva Kumar et al., 2018c; Shiva Kumar and Himabindu, 2019a; Upadhyay et al., 2020, 2022). Typical proton exchange membranes are Nafion®, Fumapem®, Flemion®, and Aciplex® respectively. However, most widely used membrane is Nafion® (Nafion® 115, 117, and 212), because Nafion® membrane offers several advantages such as high proton conductivity, possess high current density, high mechanical strength, and chemical stability respectively. The state-of-the-art anode and cathode electrode materials are noble metal based electrocatalysts especially IrO_2 for the OER and carbon-supported Pt for the HER respectively (Ramakrishna et al., 2016; Shiva Kumar et al., 2018a,d; Lee et al., 2019). These noble metals are more expensive, and iridium is scarcer than platinum. For example, a 10 MW PEM water electrolyzer operating at 1 A/cm^2 requires about 15 kg of Iridium with an assumed catalyst loading of 2–3 mg/cm^2, the expected cost of Iridium catalyst would be more than 2,941,789 US$ (196,119 US$/kg in August 2021) (Metalary, 2021). The porous titanium/titanium mesh and carbon cloth are used as anode and cathode gas diffusion layers. Different flow field designed bipolar plates made up of titanium material coated with platinum/gold are used as separators and endplates respectively. Among different flow field designs, the straight parallel flow field designed separator plates have shown better performance, especially in PEM water electrolyzer (Yang et al., 2019). However, these separator plates are expensive and are responsible for 48% of the overall cell cost (IRENA, 2020b). Therefore, the cost-effective cell components i.e., electrode materials and separator plates still under challenge.

3.3.3. Research and development of pem water electrolysis

PEM water electrolysis technology is well developed and commercially available up to megawatt (MW) for industrial and transportation applications, some of the large-scale PEM electrolyzer manufacturers are listed in Table 4. However, several improvements are still required to reduce the hydrogen production cost, the present hydrogen production cost is USD 700–1400 kW/H_2 (2020), and targeted cost reduction is USD $\leq$ 200 kW/H_2 (2050) (IRENA, 2020b). To achieve this target, the existing challenges need to be addressed such as replacement/reduction of platinum group metals with cost-effective transition metals, removing the expensive coatings on bipolar plates, and redesigning the new bipolar plates with cost-effective materials. Moreover, to reduce the membrane thickness and enhance the cell efficiency. Currently, the Nafion® 117 (thickness 180 μm) membrane is using in PEM water electrolyzers, the efficiency loss from this membrane is 25% (at 2 A/cm^2), if reducing the thickness as low as 20 μm the predicted reduction efficiency losses is 6% (at 2 A/cm^2). Therefore, in this direction several researchers from public and private organizations are still working on their developments especially focusing on cost reduction. For example, Xie et al. (2021) reported integrated electrode architectures to consist of platinum nanowires on ultrathin titanium gas diffusion layers for hydrogen evolution reaction in PEM water electrolysis. The ultrathin titanium integrated PtNW electrode (PtNW/Ti) showed a lower overpotential of 63 mV at the higher current density of 100 mA cm^{-2} with a smaller Tafel slope of 35 mV dec^{-1}. Further, electrochemical performances were studied in PEM water electrolyzer as a cathode electrode, the attained results demonstrated that the PtNW/Ti electrode has showed a lower cell voltage of 1.643 V at 1 A cm^{-2} and high efficiency of 90.08% with 15 times lower catalyst loadings than conventional MEAs in PEM water electrolysis. Also, Xie et al. (2022) developed ionomer-free integrated electrodes (1T-2H MoS_2NS/CFP) using engineered 1T-2H heterophase with MoS_2 nanosheets (MoS_2NSs) by in-situ growing on carbon fiber paper with MoS_2 loading of only 0.14 mg/cm^2 for HER and studied their performance in 0.5M H_2SO_4 as well as in PEM water electrolyzer. The integrated electrode has shown outstanding performance with an extremely lower overpotential of 192 mV and a smaller Tafel slope of 44 mV dec^{-1}. Further, the PEM water electrolyzer results exhibited that, the integrated electrode impressively achieved a cell voltage of 2.25 V at an operating current density of 2 A/cm^2, as shown in Fig. 10. Furthermore, the integrated electrode performance was

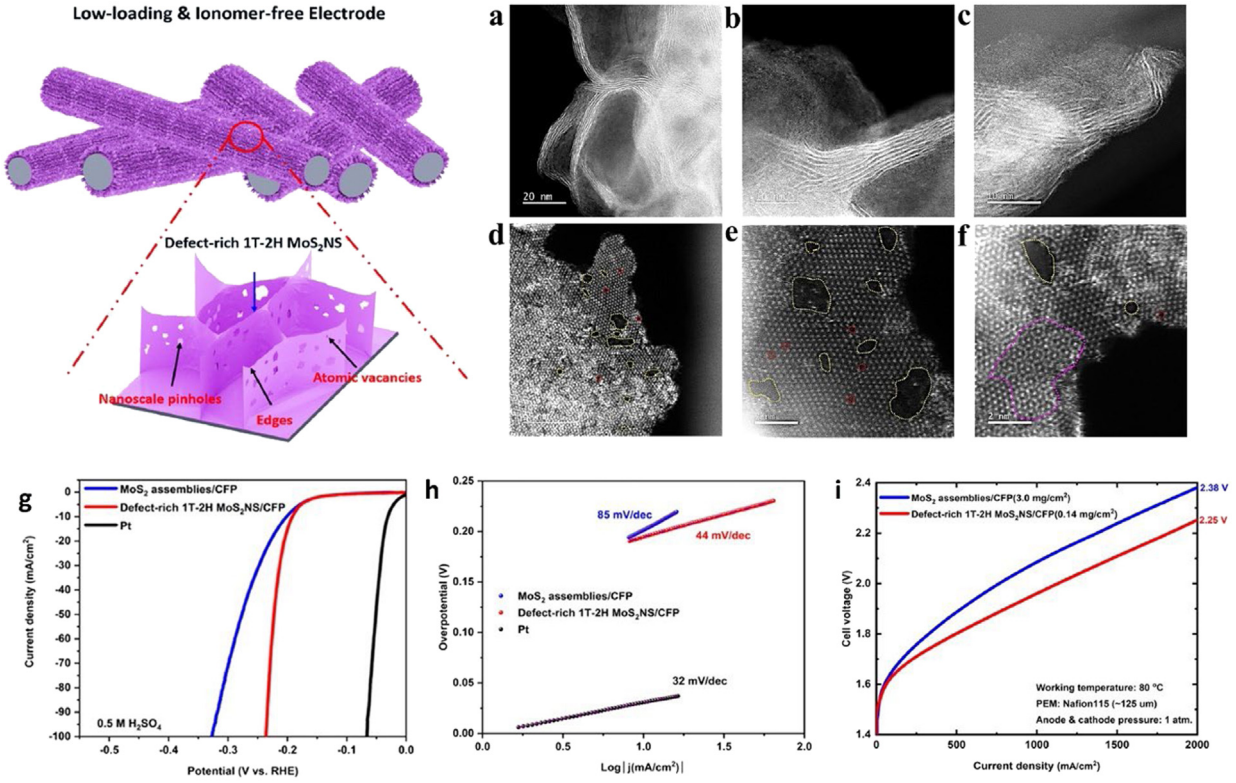

Fig. 10. Schematic illustration of Ionomer-free electrode with in-situ grown ultralow-loading and defect-rich 1T-2H MoS2 nanosheets. (a–f) HAADF-STEM images of defect-rich 1T-2H MoS2NS/CFP, confirming the co-existence of edges, pinholes & atomic vacancies. (g) Polarization curves of defect-rich 1T-2H MoS2NS/CFP and MoS2 assemblies/CFP. (h) Corresponding Tafel plots. (i) Polarization curves of defect-rich 1T-2H MoS2NS/CFP and MoS2 assemblies/CFP in a PEMEC at 80 °C (Xie et al., 2022).

compared with the commercial Pt/C catalysts with similar metal loading of 2.0 mg/cm^2. The commercial Pt/C catalyst exhibited a lower cell voltage of 2.18 V than that of the integrated 1T-2H MoS_2NS/CFP electrode (2.25 V) at the current density of 2 A cm^{-2} but this performance is superior to reported non-noble catalysts.

Jang et al. (2020a,b) introduced a novel titanium-doped molybdenum phosphide (Ti-MoP) electrocatalyst for hydrogen evolution reaction in acid electrolyte. The developed Ti-MoP electrocatalyst demonstrated superior electrochemical performance than undoped MoP with an overpotential of only 81.5 mV at 10 mA cm^{-2} than that of undoped MoP (93.5 mV) under the acidic electrolyte (0.5M H_2SO_4), indicating that the HER performance is improved approximately 13% by doping Ti with MoP. The Tafel slope also shows that Ti-MoP has a lower (44.5 mV dec^{-1}) than that of undoped (MoP 46.3 mV dec^{-1}). Further, the electrochemical stability was studied for 8000 cycles and 15 days for undoped MoP and Ti-doped MoP, the Ti-doped MoP electrocatalyst exhibited improved stability in 0.5M H_2SO_4 solution. Yoon et al. (2021) developed a platinum-free cobalt phosphide (Co-P) electrode for the hydrogen evolution reaction, the electrode was fabricated on carbon paper by pulse electrodeposition technique with various dissolution amounts of Co. The acid-dissolved Co-P-0.3 electrode showed better electrochemical performance with an overpotential of 143.85 mV at the current density of 10 mA cm^{-2} and the Tafel slope of 60.10 mV dec^{-1}. Further, the single-cell water electrolysis experiments were also carried out with Co-P-0.3 as a cathode electrode, which showed the remarkable performance, the achieved current density of 1.89 A cm^{-2} at a cell voltage of 2.0 V. Tajuddin et al. (2021) reported noble metal-free graphene-encapsulated NiMo alloy as an acid-stable catalyst for HER. The N-doped graphene (4–8 layers) encapsulated NiMo cathode catalyst exhibited an extremely stable electrochemical performance in the potential cycling test of 10,000 cycles. Moreover, exhibited highly stable electrochemical performance after the 100 h of stability test at the constant cell voltage of 2.2 V in single cell PEM water electrolyzer. Recently, Atchudan et al. (2022) developed a noble metal-free molybdenum disulfide decorated banana peel porous carbon (MoS_2@BPPC) catalyst for hydrogen evolution reaction (HER). The developed MoS_2@BPPC composite electrocatalyst showed higher HER activity and possessed superior stability in the acidic conditions (0.5M H_2SO_4) with an overpotential of 150 mV at the current density of 10 mA cm^{-2}, and the Tafel slope of 51 mV dec^{-1}. Further, Brito et al. (2022) introduced transition metal phosphide catalyst supported on carbon black (FeP/CB) for HER as an alternative to platinum-based catalysts. The prepared 50% FeP/CB catalyst showed better electrocatalytic activity with an achieved overpotential of 252 mV at the current density of 10 mA cm^{-2}, which is quite close to the 220 mV of platinum catalyst.

Jiang et al. (2021) designed Ir film decorated WO_x nanorods (Ir@WO_xNRs) through electrodeposition techniques for OER electrodes and studied their electrochemical performance in acidic media. The designed Ir@WO_xNRs electrode with reduced noble metal loading of 0.14 mg cm^{-2} demonstrated outstanding electrochemical performance and stability, the achieved current density of 2.2 A cm^{-2} at 2 V with an acceptable degradation rate of 49.7μV h^{-1} during the 1030 h stability test at a constant current density of 0.5 mA cm^{-2}. Further, Jiang et al. (2022) developed WO_3 nano-array electrode with a heterogeneous IrRu coating with different Ir/Ru ratios by facile electrodeposition approach and studied their OER activity and stability in acidic conditions. The developed $Ir_{3.2}Ru_{1.6}$@WO_3 electrode exhibited outstanding electrocatalytic activity and stability with a competitive overpotential of 245 mV at 10 mA cm^{-2}, which is lower than that of commercial IrO_2 (290 mV). Further, the single cell PEM water electrolysis results were exhibited an extremely high current

density of 4.5 A cm^{-2} at a cell voltage of 2.13 V with smaller Ir loading of 115 μg cm^{-2}. In addition, single-cell durability studies were carried out for 500 h at constant current density of 0.5 mA cm^{-2} at 80 °C, it shows that the single cell remains stable, as shown in Fig. 11.

Wang et al. (2021) have synthesized nitrogen defective graphite carbon nitride (N-CN) supported iridium oxide (IrO_2/N-CN) by two-step annealing followed by hydrothermal methods to increase the intrinsic OER activity of IrO_2 in PEM water electrolysis. The synthesized IrO_2/N-CN has showed superior mass activity (7.86 times) and specific activity (1.75 times) than bare IrO_2. Further, electrochemical performance was studied in 4 cm^2 single cell PEM water electrolyzer and the attained results demonstrated that the synthesized IrO_2/N-CN electrocatalyst exhibited superior electrochemical performance of 1.778 V at the operating current density of 1.6 A cm^{-2} which is significantly lower than that of IrO_2/CN (1.846 V) and IrO_2(1.846 V), as shown in Fig. 12. Additionally, the IrO_2/N-CN exhibited acceptable stability with a degradation rate of 63.3 μV h^{-1} during the 300 h durability test at a constant current density of 1.6 A cm^{-2}.

Min et al. (2021) have developed a high-performance IrO_x/W-TiO_2 electrocatalyst with the aim of noble metal reduction in PEM water electrolysis and studied their OER performance in half-cell and single cell compared with the undoped IrO_2. The half-cell test of IrO_x/W-TiO_2 exhibited an improved Ir mass activity than undoped IrO_2 and commercial IrO_2. The single-cell studies also were showed improved electrochemical performance and stability than unsupported IrO_x and commercial IrO_2. The achieved current density of 1 A cm^{-2} at 1.602 V with noble metal loading of less than 0.2 mg cm^{-2}. Kaya et al. (2021) have reported modified IrO_2 by introducing magnetic Fe_3O_4 to achieve the increased bubble separation during the OER in PEM water electrolysis. The attained results demonstrate that the prepared magnetized electrocatalyst (80% IrO_2-20% Fe_3O_4) achieved 15% increased current density during the linear sweep voltammetry tests and 4% increased current density in a single cell PEM electrolyzer test. Zhang et al. (2022) developed a core–shell nanostructured catalyst of Ru@Ir–O with tensile strains and incorporated oxygens introduced in the Ir shell that holds an extremely low OER overpotential of 238 mV at 10 mA cm^{-2} and lower Tafel slope of 92.6 mV dec^{-1} in acidic conditions. The developed core–shell catalyst was exhibited an outstanding 78-fold higher mass activity than commercial IrO_2 at 1.55 V in 0.5 M H_2SO_4 electrolyte. Further, Chen et al. (2022) reported a low-Ir core–shell OER electrocatalyst consisting of an intermetallic IrGa(IrGa-IMC) core and a partially oxidized Ir(IrOx) as a shell. The prepared IrGa-IMC@IrOx core–shell electrocatalysts showed a lower overpotential of 272 mV at 10 mA cm^{-2} and Tafel slope of 57.2 mV dec^{-1} with an ultra-low Ir loading of ∼20 μg cm^{-2} and a mass activity of 841 A gIr^{-1} at 1.52 V, which is 3.6 times higher than that of commercial Ir/C (232 A gIr^{-1}) catalyst.

3.4. Solid oxide water electrolysis

The solid oxide water electrolysis cell (SOEC) is one of the electrochemical conversion cells, it converts electrical energy into chemical energy. The development of solid oxide water electrolysis was begun in USA in the year of 1970s by General Electric and Brookhaven National Laboratory, followed by Dornier in Germany (Buttler and Spliethoff, 2018). Typically, the solid oxide water electrolyzer operates with water in the form of steam at high temperatures (500–850 °C) can drastically reduce the power consumption to split the water into hydrogen and oxygen consequently increase the energy efficiency (Hauch et al., 2020; Nechache and Hody, 2021; Choe et al., 2022). This improvement in energy efficiency can lead to a strong reduction in hydrogen cost due to power consumption being the main contributor to the hydrogen production cost in electrolysis (Shen et al., 2020). Apart from that, solid oxide water electrolysis offers two major advantages compared to the existing electrolysis technologies, the first one is high operating temperature which resulted in favorable thermodynamics and reaction kinetics allowing unrivaled conversion efficiencies. The second one is that solid oxide water electrolysis can be thermally integrated easily with downstream chemical synthesis i.e., the production of methanol, dimethyl ether, and ammonia (Khan et al., 2018). Moreover, the solid oxide water electrolysis does not require the use of noble metal electrocatalysts and gives high conversion efficiency. Despite these advantages, insufficient long-term stability has prevented the commercialization of solid oxide water electrolysis. As of now, the reported stability is only 20,000 h with yttria-stabilized zirconia thin electrolyte (Fang et al., 2017).

3.4.1. Working principle of solid oxide water electrolysis

Typically, solid oxide water electrolysis operates at higher temperatures with the consumption of water in the form of steam and generates green hydrogen and oxygen. During the solid oxide water electrolysis process, initially at the cathode side, the water molecule is reduced into hydrogen (H_2) and oxide ion (O^{2-}) by the addition of two electrons. The hydrogen released from the cathodic surface and the remaining oxide ion (O^{2-}) are traveled through the ion exchange membrane to the anode side. At the anode side, the oxide ions (O^{2-}) are further reduced to generate oxygen and electrons, then the produced oxygen is released from the anodic surface and the electrons are traveled through the external circuit to the cathode side by the positive attraction of the cathode. The basic working principle of solid oxide water electrolysis is shown in Fig. 13.

3.4.2. Cell components of solid oxide membrane water electrolysis

Solid oxide water electrolysis cell consists of main three components such as two porous electrodes (anode and cathode) and dense a ceramic electrolyte capable of conducting oxide ion (O^{2-}). The most used electrolyte is yttria-stabilized zirconia (YSZ), which is especially 8 mol% of yttria doped in a dense zirconium oxide-based ceramic material (cubic crystal structure stabilized by the addition of yttria), due to the yttria-stabilized zirconia electrolyte shows stable and excellent performance at higher temperatures (700–850 °C). Moreover, YSZ electrolyte having high ionic conductivity (10^{-2}–10^{-1} S cm^{-1}) is associated with good chemical and thermal stability (Nechache et al., 2014; Nechache and Hody, 2021). The state-of-the-art hydrogen (cathode) electrode material is a ceramic metal composed of YSZ and nickel (Ni-YSZ) which is a non-noble metal catalyst with high electronic conductivity (Nechache and Hody, 2021). The most widely used oxygen (anode) electrodes are perovskite materials i.e., LSCF ($La_{0.58}Sr_{0.4}Co_{0.2}Fe_{0.8}O_{3-\delta}$) and LSM ($(La_{1-x}Sr_x)_{1-y}MnO_{3-\delta}$ (Tietz et al., 2013). The LSCF is the mixed ionic electronic conductive material, which is high electrical and ionic conductivity (10^2 and 10^{-2} S cm^{-1}) along with high oxygen diffusion properties. Typically, LSM is considered reference material because it shows good performance (Wang et al., 2020a,b).

3.4.3. Research and development of solid oxide water electrolysis

The solid oxide water electrolysis technology is in the development and commercialization stage. Globally, various research institutions/organizations are actively working on the development of this technology, some of the commercial solid oxide electrolyzer manufacturers are listed in Table 4. The solid oxide water electrolysis technology offers high energy efficiency due to

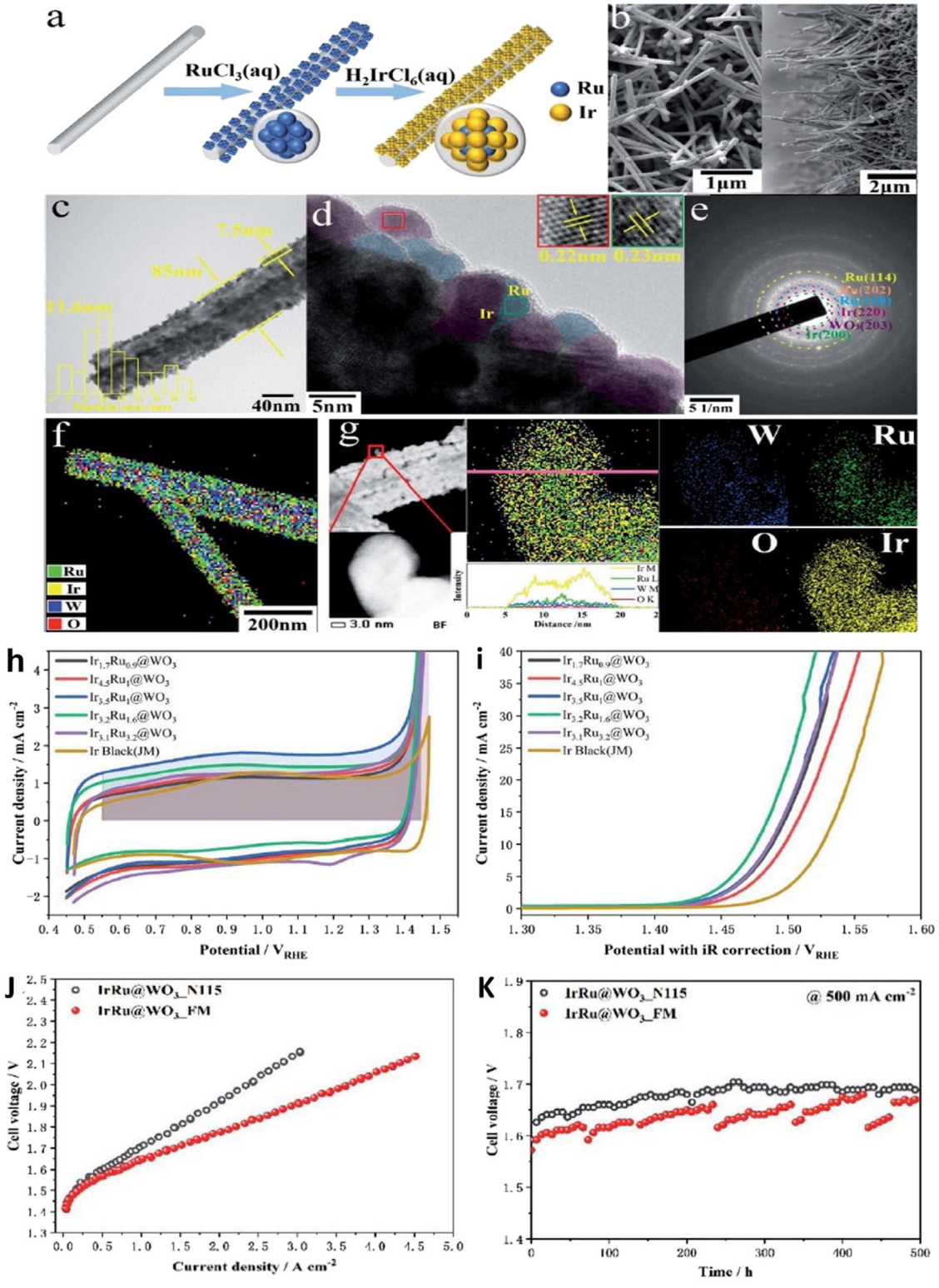

Fig. 11. Physicochemical and electrochemical performance of the developed IrRu@WO_3 nanorods. (a) A schematic illustration of the synthesis procedure of IrRu@WO_3. (b) A SEM image (left) and sectional view (right) of the array. (c) A TEM image of a single nanorod. (d) A HR-TEM image of the IrRu coating, colored blue (Ru) and purple (Ir); the inset images show magnified views of the areas in the squares. (e) A selected area electron diffraction (SAED) image. (f) A scanning TEM (STEM) image of a single nanorod with overlapping element mapping. (g) A high-angle annular dark-field (HAADF)-STEM image of a IrRu grain, elemental mapping of Ir, Ru, W and O, an overlap image, and line scanning along the pink line. (h) CV curves with a shaded area representing the OER activity and stability (i) OER LSV curves (j) Single electrolyzer I–V polarization curves at 80 °C. (k) Durability testing at 80 °C at constant current density (Jiang et al., 2022). . (For interpretation of the references to color in this figure legend, the reader is referred to the web version of this article.)

operating the higher temperatures with non-noble metal electrocatalysts. However, some of the challenges associated with this technology such as long-term stability, the present stability is 20,000 h only and the targeted stability of 1,00,000 h and hydrogen production cost, the present hydrogen production cost is USD 2000 kW/H_2 (2020), and the targeted cost reduction of USD

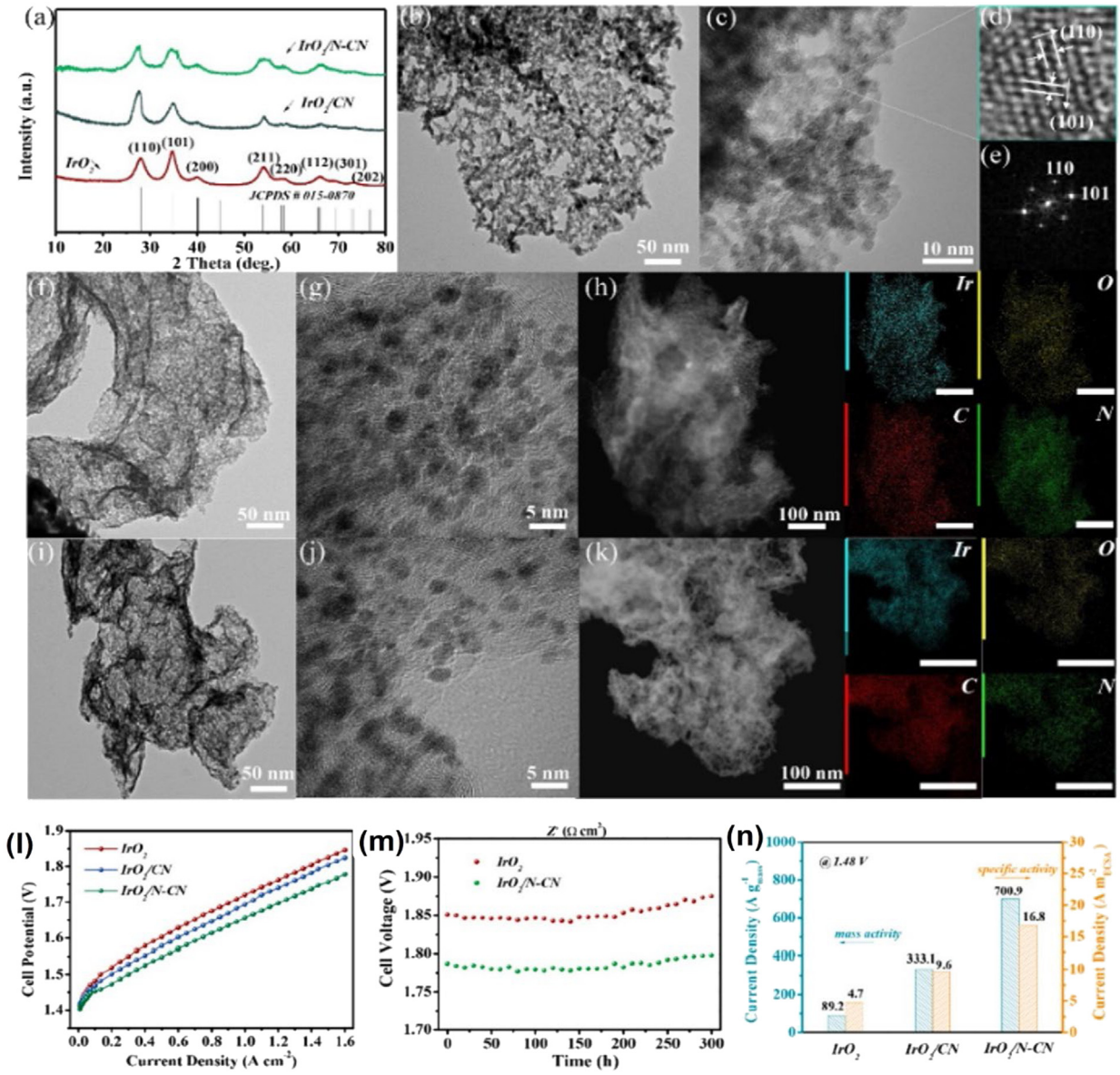

Fig. 12. (a) (a) XRD patterns; (b) TEM image, (c, d) HRTEM images and (e) corresponding FFT patterns of IrO2; (f) TEM image, (g) HRTEM image, (h) HAADF image and corresponding mapping of Ir, O, C, N element of IrO2/CN; (i) TEM image, (j) HRTEM image, (k) HAADF image and the corresponding EDX mapping of Ir, O, C, N element, of IrO2/N-CN. (*l*) I–V polarization curves (*m*) IrO2/N-CN stability for 300 h at constant current density of 1.6 A cm^2 (*n*) Mass and specific activities of IrO2, IrO2/CN and IrO2/N-CN at 12.48 V (Wang et al., 2021).

$\leq$ 200 kW/H_2 (2050) (IRENA, 2020b). To achieve these targets, the existing challenges need to be addressed such as increasing the longer-term stability by using electrochemical tuning of existing electrode materials or replacement of new perovskite materials for better stability. Apart from that, for cost reduction scaling up the electrolyzer with renewable energy sources. In this context, Li et al. (2021) have developed a composite oxide material of $Ni_{1-x}Cd_xO$-SDC and studied as the hydrogen electrode for reversible solid oxide cells. The prepared combination of R-$Ni_{0.9}Cd_{0.1}O$-SDC electrode has the most electron vacancies, resulting in the highest electrocatalytic activity during the water electrolysis and electrochemical oxidation of hydrogen. Further, the R-$Ni_{0.9}Cd_{0.1}O$-SDC electrode exhibited better electrocatalytic activity (1.4 V at 265 mA cm^{-2}) under various H_2O concentrations and the current density remain stable during the test at different voltages for a total period of 10 h under 47%H_2O + 53%H_2O atmosphere at 700 °C. Kim et al. (2021) introduced cobalt-free perovskite materials of $Ba_{1-x}Nd_xFeO_{3-\delta}$ as an oxygen electrode in solid oxide cells. The prepared $Ba_{0.97}Nd_{0.03}FeO_{3-\delta}$ has shown highest electronic conductivity (24.3 S cm^{-2}) and lowest thermal expansion coefficient (TEC) value (18.5 $\times$ 1^{-6}). In addition, the polarization resistance of $Ba_{0.97}Nd_{0.03}FeO_{3-\delta}$ has the lowest value in yttria-stabilized zirconia symmetric cells. It is due to the Nd^{3+} results in an advantage in terms of the number of additional oxygen vacancies created. More importantly, the high current density of 2.05 A cm^{-2} at 800 °C. Kim et al. (2018) reported a novel concept of hybrid solid oxide electrolysis cells (hybrid SOEC) based on the composite ionic conducting agent of $BaZr_{0.1}Ce_{0.7}Y_{0.1}Yb_{0.1}O_{3-\delta}$ which is allowing the oxygen and proton ions at the same time. The developed hybrid SOEC demonstrated the highest current density of 3.16 A cm^{-2} at 1.3 V and 700 °C with stable electrochemical stability. Zhao et al. (2021) developed a high-performance LSM-YSZ-$Ce_{0.9}Co_{0.1}O_{2-\delta}$ oxygen electrode by infiltration method and studied for hydrogen production through solid oxide electrolysis cells. The developed oxygen electrode exhibited excellent performance of 1.26 A cm^{-2} at

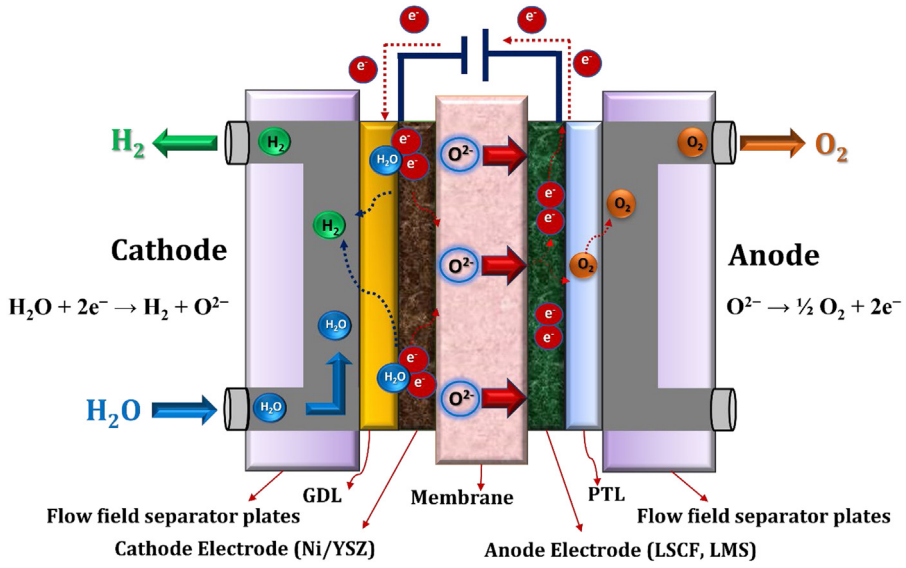

Fig. 13. Schematic view of solid oxide water electrolysis working principle.

1.3 V, which is 3.3 times higher than the blank LSM-YSZ electrode. Additionally, higher hydrogen generation rate of 873 mL cm^{-2} h^{-1}. Zheng et al. (2021) introduced a novel electrode material of Mn-doped Ruddlesden–Popper oxide $La_{1.5}Sr_{0.5}NiO_{4+\delta}$ ($LSNM_x$) and their performance was evaluated in solid oxide electrolyzer as an oxygen electrode. The $LSNM_{0.5}$ showed lower resistance of 0.488 Ω cm^2 at 800 °C with a current density of 500 mA cm^{-2} at 1.4 V at 800 °C with stable electrocatalytic activity during the 145 h continuous operation, as shown in Fig. 14. This current density is 85.2% higher than the un-doped LSN electrode.

Vibhu et al. (2021) developed layered perovskite-based rare earth nickelates of $Ln_2NiO_{4+\delta}$ (Ln = La, Pr, and Nd) as an alternative OER electrode for high-temperature solid oxide electrolysis cells. Among all the synthesized nickelate electrodes, the $Pr_2NiO_{4+\delta}$ (PNO) showed better electrochemical performance but it showed a relatively higher degradation rate of 88 mV h^{-1} at higher current densities. Further, increased the $Pr_2NiO_{4+\delta}$ electrode durability by substitution of cobalt. The modified cobalt substituted $Pr_2Ni_{0.8}Co_{0.2}O_{4+\delta}$ electrode were showed improved electrochemical performance and stability at higher current densities, the achieved maximum current density of 3.0 A cm^{-2} and 1.9 A cm^{-2} at a cell voltage of 1.5 V at 900 °C and 800 °C with a lower degradation rate of 22 mV kh^{-1} in single-cell studies of 250 h at the constant current density of −1 A cm^{-2} at 800 °C with 50% H_2 and H_2O feed gas mixture, as shown Fig. 15 (Vibhu et al., 2021).

Further, Kukk et al. (2021) studied the long-term stability of different electrode materials such as Ni-$Zr_{0.92}Y_{0.08}O_{2-\delta}$| $Zr_{0.92}Y_{0.08}O_{2-\delta}$| $Ce_{0.9}Gd_{0.1}O_{2-\delta}$| $Pr_{0.6}Sr_{0.4}CoO_{3-\delta}$ in solid oxide fuel cells (SOFC) for 17,820 h at 650 °C and solid oxide electrolysis cells (SOEC) for 860 h at 800 °C. The attained results show that the $Pr_{0.6}Sr_{0.4}CoO_{3-\delta}$ electrocatalyst has shown better stability in SOFC with a small degradation rate of 2.4% for the first 1000 h and 1.1% for later, the degradation is mainly due to the formation of silicon and chromium impurities on the electrolyte. During the SOEC studies, the observed degradation rate of 16.3%, this higher degradation was due to the formation of silicon and chromium impurities along with cracks on the electrode.

4. Recommendations for future research and development

Green hydrogen production from renewable energy sources like wind and solar using water electrolysis technology is expected to be at the heart of the energy transition to meet the net-zero challenges. In addition, water electrolysis is a well-known electrochemical process for green hydrogen production that requires wider adoption to lower production costs with high efficiency. Therefore, essential improvements and innovations are required to produce viable green hydrogen and meet the global net-zero challenges. In this context, various water electrolysis technologies and their challenges, and possible solutions are given below for cost reduction and commercialization perspective.

Alkaline water electrolysis

Alkaline water electrolysis is well established and mature technology for green hydrogen production. However, some of the challenges associated with alkaline water electrolysis such as lower operating current density, cell efficiency, and crossover of the gases. Therefore, some improvements/developments are needed in this technology.

- Separators (Diaphragms) — The thickness of the diaphragms can be reduced with lower resistance this can improve the cell efficiency and reduce the electricity consumption. The overall thickness of the diaphragms should be reached 50 μm than the present thickness of ∼460 μm, this would be contributed to improving the cell efficiency from 53% to 75% at 1 A/cm^2.
- Current density — The lower current density is one of the major barriers to alkaline water electrolysis, the significant innovations/improvements are needed to increase the current density. The current density should be reached up to 2–3 A/cm^2 than the present current density of 0.8 A/cm^2. This can be achieved by using the thinner diaphragms with high specific surface area electrode materials.
- Crossover of the gasses — Typically alkaline water electrolysis takes place on the high concentrated (5M) KOH electrolyte and high thickness diaphragms with nickel-based electrodes. During the electrochemical reaction, this can allow the intermixing of the generated gases, which are dissolved into the electrolyte subsequently producing the low purity of the gases. To reduce this crossover of the gasses can be achieved by reducing the thickness of the diaphragms. In addition, reducing the interface resistances between catalyst layers and porous transport layers.

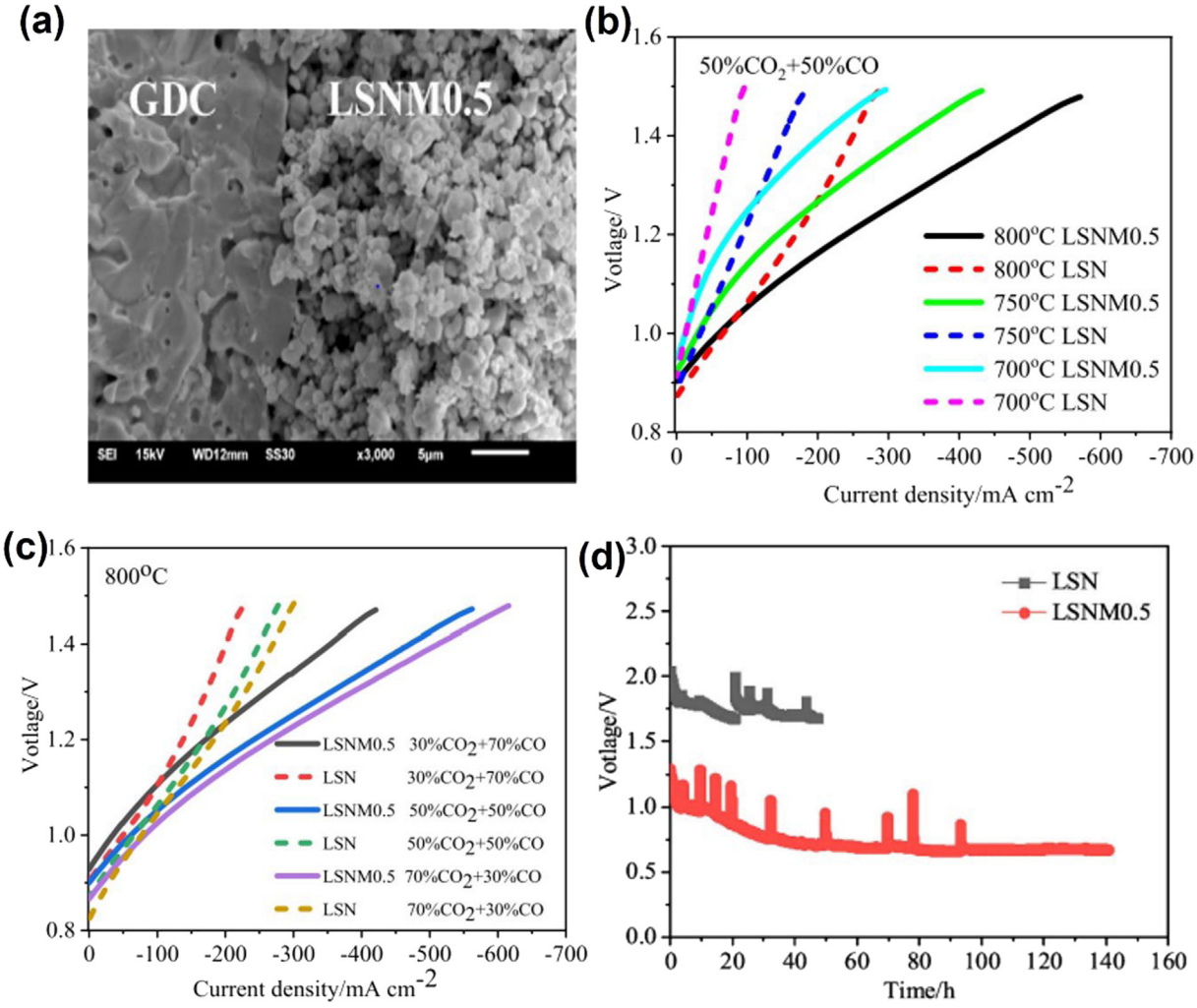

Fig. 14. (a) SEM micrographs of GDC/LSNM0.5 (b) Current–voltage polarization curves of LSNM0.5 and LSN in single cell with 50% CO_2+50% CO as feed gas at different temperatures (c) Current–voltage polarization curves of LSNM0.5 and LSN in single cell with different gases fed into the fuel electrode at 800 °C. (d) Electrolysis stability studies of LSNM0.5 and LSN at 800 °C (Zheng et al., 2021).

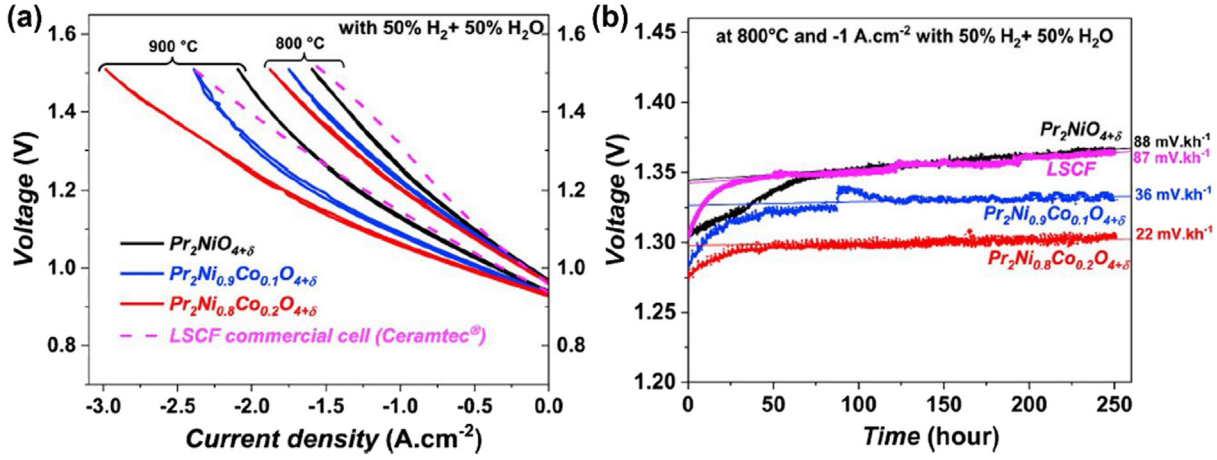

Fig. 15. (a). Current–voltage polarization curves of $Pr_2NiO_{4+\delta}$, $Pr_2Ni_{0.9}Co_{0.1}O_{4+\delta}$, $Pr_2Ni_{0.8}Co_{0.2}O_{4+\delta}$, and LSCF electrodes at 800 and 900°C in SOEC single cell (b) Long-term stability of $Pr_2NiO_{4+\delta}$, $Pr_2Ni_{0.9}Co_{0.1}O_{4+\delta}$, $Pr_2Ni_{0.8}Co_{0.2}O_{4+\delta}$, and LSCF electrodes at 800 °C at constant current density of −1 A cm^{-2} at 800 °C (Vibhu et al., 2021).

Table 4
Global leading electrolyzer manufacturers and their specifications.

Alkaline water electrolysis						
Manufacture	Origin of Country	Generic name	H_2 Capacity (N m^3/h)	Pressure (bar)	Energy consumption (kWh/N m^3)	Ref.
Nel.	Norway	A3880	2400–3880	200	3.8–4.4	Nel
Cummins	Canada	HySTAT® -100–10	100	10	5.0–5.4	Cummins
John Cockerill	Belgium	DQ-500	500	30	4.0–4.3	John Cockerill
McPhy	France	MeLyzer 800–30	800	30	4.5	McPhy
Sunfire	Germany	HyLink Alkaline	2230	30	4.7	Sunfire
Nuberg PERIC	China–India	ZDQ-600	600	20	4.6	Nuberg PERIC
TIANJIN Mainland	China	FDQ800	1000	5	4.4	TIANJIN Mainland
GreenHydrogen	Denmark	HyProvide A-90	90	35	4.3	Green hydrogen Systems,
AEM water electrolysis						
Enapter	Germany	AEM Multicore	210	35	4.8	Enapter,
PEM water electrolysis						
Nel.	Norway	M5000	5000	30	4.5	Nel
Cummins	Canada	HyLYZER® -4.000-30	4000	30	4.3	Cummins
Siemens	Germany	Silyzer 300	100–2000	35	N/A	Siemens
Proton onsite	USA	M400	417	30	N/A	Proton onsite
ITM Power	UK	HGASXMW	110–1900	20	N/A	ITM Power
Plug Power	USA	GenFuel 5 MW	1000	40	5.2	Plug Power
Elogen	France	ELYTE 260	260	30	4.9	Elogen
Solid oxide water electrolysis						
Sunfire	Germany	HyLink SOEC	750	40	3.6	Sunfire

AEM water electrolysis

AEM water electrolysis is the latest developing technology, this technology is introduced to overcome the drawbacks of alkane and PEM water electrolysis. However, the major challenge associated with this technology is limited stability.

- Membranes and Ionomers — membrane durability is one of the major challenges to scaling up this technology, the present membrane's durability is around 30,000 h only due to the polymer degradation from the membrane backbone chain (chemically unstable). Therefore, considerable improvements/innovations are required to increase the durability and overcome the polymer degradation, this can be achieved by increasing the chemical, mechanical and thermal stability of the membranes along with increasing the ionic conductivity using high conducting polymer compositions. In addition, improve the electrode kinetics for OER and HER by tuning the metal surfaces, to maintain the long-term stability.

PEM water electrolysis

PEM water electrolysis offers several advantages over alkaline water electrolysis such as high operating current density, high purity of gases, higher outlet pressure, and smaller footprint. However, the major challenge associated with this technology is cost of the components. Therefore, considerable developments are needed to reduce the cost.

- Membranes — The membrane is a key component of the PEM water electrolyzer and significant innovation/improvements are needed in this area to increase the efficiency and durability and reduce the cost. For example, reducing the membrane thickness with stronger mechanical resistance enables an increase in efficiency and durability, which in turn enables a reduction in electricity consumption.
- Electrocatalyst Materials — Electrocatalysts are another key component of PEM electrolyzer and significant innovations are required in this area due to the precious materials (Pt/IrO_2) being a major barrier to PEM electrolyzer cost and scale-up. Therefore, significant solutions to replace/reduce such materials are essential, this can be achieved by using earth-abundant non-noble materials. In addition, reduction of precious materials loadings with increase in the kinetics of OER and HER electrode materials by tuning the surface properties like increasing the surface area.
- Stackability (Electrolyzer cell stack) — Porous transport layers and bipolar plates contribute a significant ratio to the overall stack cost due to the use of platinum or gold-coated titanium materials. Therefore, significant innovations are needed in these components, including their design and manufacturing, which can enable lower system costs.

Solid oxide water electrolysis

Solid oxide water electrolysis is a developing technology with high efficiency. However, the main challenge is durability, so significant advancements are essential for this area to increase the durability.

- Durability — The improved durability can be achieved by increasing the electrolyte conductivity and optimization of chemical and mechanical stability. In addition, tuning the electrochemical surface properties and compatibility of the electrode materials, for example, control the nickel agglomeration or oxidation state of OER electrodes and the lanthanum manganite (LSM) or lanthanum ferrite (LSF) delamination from the electrolyte.

5. Conclusions

Nowadays rapidly growing interest in water electrolysis technologies is because green hydrogen production is the most promising renewable energy vector for global decarbonization. However, green hydrogen production is limited to demonstration projects due to economic issues. In this review, a brief introduction was made about the various water electrolysis technologies and their techno-commercial prospects including hydrogen production cost, along with recent developments in electrode materials, and their challenges. In addition, some of the most successful results also were described and identified the research gaps in water electrolysis research and development towards the commercialization prospects. However, as of now the green hydrogen production cost is high compared to the conventional blue hydrogen production cost because of the use of expensive materials. Therefore, in order to reduce the green hydrogen cost, we outlined our ideas, possible solutions, and recommendations in the direction the future research should proceed to develop efficient

and cost-effective water electrolysis technologies to mitigate the environmental and economic concerns.

Declaration of competing interest

The authors declare that they have no known competing financial interests or personal relationships that could have appeared to influence the work reported in this paper.

Data availability

No data was used for the research described in the article.

Acknowledgments

This research was supported by the Hydrogen Energy Innovation Technology Development Program of the National Research Foundation of Korea (NRF) funded by the Korean government (Ministry of Science and ICT (MSIT)) (NRF-2019M3E6A1064290), the National Research Foundation of Korea (NRF) grant funded by the Korea government (NRF- 2019M1A2A2065614), and the Carbon Neutrality Demonstration and Research Center of UNIST (Ulsan National Institute of Science and Technology).

References

Ajanovic, A., Sayer, M., Haas, R., 2022. The economics and the environmental benignity of different colors of hydrogen. Int. J. Hydrogen Energy http://dx.doi.org/10.1016/j.ijhydene.2022.02.094, Accepted 11 2022.

Atchudan, R., Perumal, S., Jebakumar Immanuel Edison, T.N., Aldawood, S., Vinodh, R., Sundramoorthy, A.K., Ghodake, G., Lee, Y.R., 2022. Facile synthesis of novel molybdenum disulfide decorated banana peel porous carbon electrode for hydrogen evolution reaction. Chemosphere 307, 135712.

Bertuccioli, L., Chan, A., Hart, D., Lehner, F., Madden, B., Standen, E., 2014a. Development of Water Electrolysis in the European Union. In: Element Energy, E4tech Sarl, Cambridge (UK), Lausanne (CH, 2014.

Bertuccioli, L., Chan, A., Hart, D., Lehner, F., Madden, B., Standen, E., 2014b. Study on development of water electrolysis in the EU. In: Fuel Cells and Hydrogen Joint Undertaking. Final report.

Brauns, J., Thomas, T., 2020. Alkaline water electrolysis powered by renewable energy: A review. Processes 8, 248.

Brito, J., Restivo, J., Sousa, J.P.S., Spera, N.C.M., Falcao, D.S., Rocha, A., Pinto, A.M.F.R., Pereira, M.F.R., Soares, O.S.G.P., 2022. Implementation of transition metal phosphides as pt-free catalysts for PEM water electrolysis. Energies 15, 1821.

Burton, N.A., Padilla, R.V., Rose, A., Habibullah, H., 2021. Increasing the efficiency of hydrogen production from solar powered water electrolysis. Renew. Sustain. Energy Rev. 135, 110255.

Buttler, A., Spliethoff, H., 2018. Current status of water electrolysis for energy storage, grid balancing and sector coupling via power-to-gas and power-to-liquids: A review. Renew. Sustain. Energy Rev. 82, 2440–2454.

Carbone, A., Zignani, S.C., Gatto, I., Trocino, S., Arico, A.S., 2020. Assessment of the FAA3-50 polymer electrolyte in combination with a $NiMn_2O_4$ anode catalyst for anion exchange membrane water electrolysis. Int. J. Hydrog. Energy 45, 9285–9292.

Carmo, M., Fritz, D.L., Mergel, J., Stolten, D., 2013. A comprehensive review on PEM water electrolysis. Int. J. Hydrogen Energy 38, 4901–4934.

Chen, L-W., He, F., Shao, R-Y., Yan, Q-Q., Yin, P., Zeng, W-J., Zuo, M., He, L., Liang, H-W., 2022. Intermetallic IrGa-IrO_x core–shell electrocatalysts for oxygen evolution. Nano Res. 15, 1853–1860.

Chen, N., Paek, S.Y., Lee, J.Y., Park, J.H., Lee, S.Y., Lee, Y.M., 2021. High-performance anion exchange membrane water electrolyzers with a current density of 7.68 A cm^{-2} and a durability of 1000 h. Energy Environ. Sci. 14, 6338–6348.

Choe, C., Cheon, S., Gu, J., Lim, H.K., 2022. Critical aspect of renewable syngas production for power-to-fuel via solid oxide electrolysis: integrative assessment for potential renewable energy source. Renew. Sustain. Energy Rev. 161, 112398.

Cummins, ., 2022. HySTAT® -100-10. Technical Specifications, https://www.cummins.com/sites/default/files/2021-08/cummins-hystat-100-specsheet.pdf (Accessed 28 August 2022).

David, M., Ocampo-Martinez, C., Sanchez-Pena, R., 2019. Advances in alkaline water electrolyzers: A review. J. Energy Storage 23, 392–403.

Dawood, F., Martin, A., Shafiullah, G.M., 2020. Hydrogen production for energy: An overview. Int. J. Hydrog. Energy 45, 3847–3869.

Diogo, M.F., SantosCésar, A.C., SequeiraJose, L., Figueiredo, ., 2013. Hydrogen production by alkaline water electrolysis. Quim. Nova 36, 1176–1193.

EIA, ., 2016. U.S. Energy Information Administration 2016. Monthly Energy Review. DOE/EIA-0035(2016/04), https://www.eia.gov/totalenergy/data/monthly/pdf/mer.pdf.

Elogen, ., 2021. PEM electolyser. France, https://elogenh2.com/wp-content/uploads/2021/04/Elogen_Product_sheet-Elyte260.pdf (Accessed 13 August 2021).

Enapter, ., 2022. AEM Multicore Datasheet. Germany, https://handbook.enapter.com/electrolyser/aem_multicore/downloads/Enapter_Datasheet_AEM-Multicore_EN_COM.pdf (Accessed 28 August 2022).

Fang, Q., Blum, L., Menzler, N.H., Stolten, D., 2017. Solid oxide electrolyzer stack with 20, 000 h of operation. ECS Trans. 78, 2885–2893.

2021. Green hydrogen Systems. In: HyProvide a-Series, Denmark, https://greenhydrogen.dk/wp-content/uploads/2021/02/A-Series-brochure-120421.pdf (Accessed 13 August 2021).

Grigoriev, S.A., Fateev, V.N., Bessarabov, D.G., Millet, P., 2020. Current status, research trends, and challenges in water electrolysis science and technology. Vol. 45, pp. 26036-26058.

Guo, W., Kim, J., Kim, H., Ahn, H.S., 2021. Cu-Co-P electrodeposited on carbon paper as an efficient electrocatalyst for hydrogen evolution reaction in anion exchange membrane water electrolyzers. Int. J. Hydrog. Energy 46, 19789–19801.

Hall, W., Spencer, T., Renjith, G., Dayal, S., 2020. The Potential Role of Hydrogen in India: A Pathway for Scaling-Up Low Carbon Hydrogen Across the Economy. The Energy and Resources Institute (TERI), New Delhi.

Hauch, A., Kungas, R., Blennow, P., Hansen, A.B., Hansen, J.B., Mathiesen, B.V., Mogensen, M.B., 2020. Recent advances in solid oxide cell technology for electrolysis. Science 370, eaba6118.

Henkensmeier, D., Najibah, M., Harms, C., Zitka, J., Hnat, J., Bouzek, K., 2021. Overview: State-of-the art commercial membranes for anion exchange membrane water electrolysis. J. Electrochem. En. Conv. Storage 18, 024001.

Hermesmann, M., Muller, T.E., 2022. Green, turquoise, blue, or grey? Environmentally friendly hydrogen production in transforming energy systems. Prog. Energy Combust. Sci. 90, 100996.

Ibrahim, D., 2012. Green methods for hydrogen production. Int. J. Hydrog. Energy 37, 1954–1971.

IEA, ., 2019a. Statistics, global primary energy demand by fuel, 1925–2019. (Accessed 13 2022).

IEA, ., 2019b. The future of hydrogen. https://www.hydrogenexpo.com/media/9370/the_future_of_hydrogen_iea.pdf.

IEA, ., 2021. Global hydrogen review. https://www.iea.org/reports/global-hydrogen-review-2021.

Immanuel, V., Dmitri, B., 2018. Low-cost hydrogen production by anion exchange membrane electrolysis: A review. Renew. Sustain. Energy Rev. 81, 1690–1704.

Ionomr, 2020. WHITE PAPER: Hydrogen Production Cost by AEM Water Electrolysis. Document ID: FM-7024-B, Ionomr Innovations Inc.

IRENA, ., 2020a. Green Hydrogen: A Guide to Policy Making. International Renewable Energy Agency, Abu Dhabi, ISBN: 978-92-9260-286-4.

IRENA, ., 2020b. Green Hydrogen Cost Reduction: Scaling Up Electrolysers to Meet the 1.5 °C Climate Goal. International Renewable Energy Agency, Abu Dhabi, ISBN: 978-92-9260-295-6.

ITM Power, 2021. HGasXMW. Accessed 13 2021.

Jacquet, J., Jamieson, D., 2016. Soft but significant power in the Paris agreement. Nature Clim. Change 67, 643–646.

Jang, I., Im, K., Shin, H., Lee, K-S., Kim, H., Kim, J., Yoo, S.J., 2020a. Electron-deficient titanium single-atom electrocatalyst for stable and efficient hydrogen production. Nano Energy 78, 105151.

Jang, M.J., Yang, J., Lee, J., Park, Y., Jeong, J.H., Park, S., Jeong, J., Yin, Y., Seo, M., Choi, S.M., Lee, K.H., 2020b. Superior performance and stability of anion exchange membrane water electrolysis: pH-controlled copper cobalt oxide nanoparticle for oxygen evolution reaction. J. Mater. Chem. A 8, 4290–4299.

Jiang, G., Yu, H., Li, Y., Yao, D., Chi, J., Sun, S., Shao, Z., 2021. Low-loading and highly stable membrane electrode based on an ir@woxnr ordered array for PEM water electrolysis. ACS Appl. Mater. Interfaces 13, 15073–15082.

Jiang, G., Yu, H., Yao, D., Li, Y., Chi, J., Zhang, H., Shao, Z., 2022. Boosting the oxygen evolution stability and activity of a heterogeneous IrRu bimetallic coating on a wo_3 nano-array electrode for PEM water electrolysis. J. Mater. Chem. A 10, 11893.

Jin, Z., Wang, L., Chen, T., Liang, J., Zhang, Q., Peng, W., Li, Y., Zhang, F., Fan, X., 2021. Transition metal/metal oxide interface (Ni-Mo-O/Ni_4mo) stabilized on N-doped carbon paper for enhanced hydrogen evolution reaction in alkaline conditions. Ind. Eng. Chem. Res. 60, 5145–5150.

John Cockerill, ., 2021. DQ500 alkaline electrolyser. https://h2.johncockerill.com/wp-content/uploads/2022/02/DQ-500-def-hd.pdf (Accessed 13 August 2021).

Jovan, D.J., Dolanc, G., 2020. Can green hydrogen production be economically viable under current market conditions. Energies 13, 6599.

Kaya, M.F., Demir, N., Rees, N.V., Ahmad, E-K., 2021. Magnetically modified electrocatalysts for oxygen evolution reaction in proton exchange membrane (PEM) water electrolyzers. Int. J. Hydrog. Energy 46, 20825–20834.

Khan, M.A., Zhao, H., Zou, W., Chen, Z., Cao, W., Fang, J., Xu, J., Zhang, L., Zhang, J., 2018. Recent progresses in electrocatalysts for water electrolysis. Electrochem. Energy Rev. 1, 483–530.
Kim, J., Jun, A., Gwon, O., Yoo, S., Liu, M., Shin, J., Lim, T-H., Kim, G., 2018. Hybrid-solid oxide electrolysis cell: A new strategy for efficient hydrogen production. Nano Energy 44, 121–126.
Kim, Y-D., Yang, J-Y., Saqib, M., Park, K., Shin, J-S., Jo, M., Park, K.M., Lim, H-T., Song, S-J., Park, J-Y., 2021. Cobalt-free perovskite $Ba_{1-x}Nd_xFeO_{3-\delta}$ air electrode materials for reversible solid oxide cells. Ceram. Int. 47, 7985–7993.
Kuckshinrichs, W., Ketelaer, T., Koj, JC., 2017. Economic analysis of improved alkaline water electrolysis. Front. Energy Res. 5, 1. http://dx.doi.org/10.3389/fenrg.2017.00001.
Kukk, F., Moller, P., Kanarbik, R., Nurk, G., 2021. Study of long-term stability of Ni-$zr_{0.92}Y_{0.08}O_{2-\delta}$| $Zr_{0.92}Y_{0.08}O_{2-\delta}$| $Ce_{0.9}Gd_{0.1}O_{2-\delta}$| $Pr_{0.6}Sr_{0.4}CoO_{3-\delta}$ at SOFC and SOEC mode. Energies 14, 824.
Lee, B., Cho, H-S., Kim, H., Lim, D., Cho, W., Kim, C-H., Lim, H.K., 2021a. Integrative techno-economic and environmental assessment for green H_2 production by alkaline water electrolysis based on experimental data. J. Environ. Chem. Eng. 9, 106349.
Lee, B., Heo, J., Kim, S., Sung, C., Moon, C., Moon, S., Lim, H.K., 2018. Economic feasibility studies of high-pressure PEM water electrolysis for distributed H_2 refuelling stations. Energy Convers. Manage. 162, 139–144.
Lee, H., Lee, B., Byun, M., Lim, H.K., 2020. Economic and environmental analysis for PEM water electrolysis based on replacement moment and renewable electricity resources. Energy Convers. Manage. 224, 113477.
Lee, B., Lee, H., Heo, J., Moon, C., Moon, S., Lim, H.K., 2019. Stochastic techno-economic analysis of H_2 production from power-to-gas using a high-pressure PEM water electrolyzer for small-scale H_2 fueling station. Sustain. Energy Fuels 3, 2521–2529.
Lee, B., Lim, D., Lee, H., Lim, H.K., 2021b. Which water electrolysis technology is appropriate?: Critical insights of potential water electrolysis for green ammonia production. Renew. Sustain. Energy Rev. 143, 110963.
Li, P., Dong, R., Yang, P., Maa, X., Yan, F., Zhang, P., Fu, D., 2021. Performance enhanced of $NiCe_{0.8}Sm_{0.2}O_{1.9}$ hydrogen electrode for reversible solid oxide cells with cadmium substitution. J. Electroanal. Chem. 882, 115018.
Lim, D., Lee, B., Lee, H., Byun, M., Cho, H-S., Cho, W., Kim, C-H., Boris, B., Lim, H.K., 2021. Impact of voltage degradation in water electrolyzers on sustainability of synthetic natural gas production: Energy, economic, and environmental analysis. Energy Convers. Manage. 245, 114516.
Liu, S., Li, B., Mohite, S.V., Devaraji, P., Mao, L., Xing, R., 2020. Ultrathin MoS_2 nanosheets in situ grown on rich defective $Ni_{0.96}S$ as heterojunction bifunctional electrocatalysts for alkaline water electrolysis. Int. J. Hydrog. Energy 45, 29929–29937.
Lv, Z., Ma, W., Wang, M., Dang, J., Jian, K., Liu, D., Huang, D., 2021. Co-constructing interfaces of multiheterostructure on mxene ($Ti_3C_2T_x$)-modified 3D self-supporting electrode for ultraefficient electrocatalytic HER in alkaline media. Adv. Funct. Mater. 31, 2102576.
McPhy, Melyzer 800-30 electrolyser. France, Accessed 13 August 2021, 2021.
Metalary, ., 2021. Irridium price, 6100 USD per troy oz. https://www.metalary.com/iridium-price/ (Accessed 13 August 2021).
Milani, D., Ali, K., Robbie, M.N., 2020. Renewable-powered hydrogen economy from Australia's perspective. Int. J. Hydrog. Energy 45, 24125–24145.
Miller, H.A., Bouzek, K., Hnat, J., Loos, S., Bernacker, C.I., Weizgarber, T., Rontzsch, L., Meier-Haack, JJ., 2020. Green hydrogen from anion exchange membrane water electrolysis: a review of recent developments in critical materials and operating conditions. Sustain. Energy Fuels 4, 2114.
Min, X., Shi, Y., Lu, Z., Shen, L., Ogundipe, T.O., Gupta, P., Wang, C., Guo, C., Wang, Z., Tan, H., Mukerjee, S., Yan, C., 2021. High performance and cost-effective supported IrOx catalyst for proton exchange membrane water electrolysis. Electrochim. Acta 385, 138391.
Mosca, L., et al., 2020. Process design for green hydrogen production. Int. J. Hydrog. Energy 45, 7266–7277.
Mostafa, E-S., Shinji, K., Yukio, H., 2019. Hydrogen production technologies overview. J. Power Energy Eng. 7, 107–154.
Navas-Anguita, Z., Garcia-Gusano, D., Dufour, J., Iribarren, D., 2021. Revisiting the role of steam methane reforming with CO_2 capture and storage for long-term hydrogen production. Sci. Total Environ. 771, 145432.
Nechache, A., Cassir, M., Ringuede, A., 2014. Solid oxide electrolysis cell analysis by means of electrochemical impedance spectroscopy: a review. J. Power Sources 258, 164–181.
Nechache, A., Hody, S., 2021. Alternative and innovative solid oxide electrolysis cell materials: A short review. Renew. Sustain. Energy Rev. 149, 111322.
Nel, 2021a. Electrolyser technical datasheet. https://nelhydrogen.com/product/atmospheric-alkaline-electrolyser-a-series/ (Accessed 13 August 2021).
Nel, 2021b. PEM Electrolyser. In: M Series, Norway, https://nelhydrogen.com/product/m-series-3/ (Accessed 13 August 2021).
Nikolaidis, P., Poullikkas, A., 2017. A comparative overview of hydrogen production processes. Renew. Sustain. Energy Rev. 67, 597–611.
Noussan, M., Raimondi, P.P., Scita, R., Hafner, M., 2021. The role of green and blue hydrogen in the energy transition—A technological and geopolitical perspective. Sustainability 13, 298.
Nuberg PERIC, 2022. Nuberg PERIC. https://www.nubergindia.com/nuberg-hydrogen-brochure.pdf (Accessed 28 August 2022).
Pavel, C.C., Cecconi, F., Emiliani, C., Santiccioli, S., Scaffidi, A., Catanorchi, S., Comotti, M., 2014. Highly efficient platinum group metal free based membrane-electrode assembly for anion exchange membrane water electrolysis. Angew. Chem. Int. Ed. 53, 1378–1381.
Pinsky, R., Sabharwall, P., Hartvigsen, J., Brien, O.J., 2020. Comparative review of hydrogen production technologies for nuclear hybrid energy systems. Prog. Nucl. Energy 123, 103317.
2021. Plug Power USA. GENFUEL, https://www.plugpower.com/wp-content/uploads/2020/10/2021_5MWELX_Spec_F061021_1.pdf (Accessed 13 August 2021).
Proton onsite, 2021. M Series Hydrogen Generation Systems. USA, https://www.protononsite.com/sites/default/files/2017-04/PD-0600-0119%20REV%20A.pdf (Accessed 13 August 2021).
Pushkareva, I.V., Pushkarev, A.S., Grigoriev, S.A., Modisha, P., Bessarabov, D.G., 2020. Comparative study of anion exchange membranes for low-cost water electrolysis. Int. J. Hydrog. Energy 45, 26070–26079.
Qazi, U.Y., Javaid, R., Zahid, M., Tahir, N., Afzal, A., Lin, X-M., 2021. Bimetallic NiCo–$NiCoO_2$ nano-heterostructures embedded on copper foam as a self-supported bifunctional electrode for water oxidation and hydrogen production in alkaline media. Int. J. Hydrog. Energy 46, 18936–18948.
Ramakrishna, S.U.B., Srinivasulu Reddy, S., Himabindu, V., 2016. Nitrogen doped CNTs supported palladium electrocatalyst for hydrogen evolution reaction in PEM water electrolyser. Int. J. Hydrog. Energy 41, 20447–20454.
Sazal, N., 2020. Emerging technologies by hydrogen: A review. Int. J. Hydrog. Energy 45, 18753–18771.
Schmidt, O., Gambhir, I., Hawkes, A., Nelson, J., Few, S., 2017. Future cost and performance of water electrolysis: An expert elicitation study. Int. J. Hydrog. Energy 42, 30470–30492.
Shen, F., Wang, R., Tucker, M.C., 2020. Long term durability test and post mortem for metal-supported solid oxide electrolysis cells. J. Power Sources 474, 228618.
Shiva Kumar, S., Himabindu, V., 2019a. Hydrogen production by PEM water electrolysis – A review. Mater. Sci. Energy Technol. 2, 442–454.
Shiva Kumar, S., Himabindu, V., 2020. Boron-doped carbon nanoparticles supported palladium as an efficient hydrogen evolution electrode in PEM water electrolysis. Renew. Energy 146, 2281–2290.
Shiva Kumar, S., Ramakrishna, S.U.B., Bhagawan, D., Himabindu, V., 2018a. Preparation of $Ru_xPd_{1-x}O_2$ electrocatalysts for the oxygen evolution reaction (OER) in PEM water electrolysis. Ionics 24, 2411–2419.
Shiva Kumar, S., Ramakrishna, S.U.B., Naga Mahesh, K., Rama Devi, B., Himabindu, V., 2019b. Palladium supported on phosphorus–nitrogen dual-doped carbon nanoparticles as cathode for hydrogen evolution in PEM water electrolyser. Ionics 25, 2615–2625.
Shiva Kumar, S., Ramakrishna, S.U.B., Rama Devi, B., Himabindu, V., 2018c. Phosphorus doped carbon nanoparticles supported palladium electrocatalyst for the hydrogen evolution reaction (HER) in PEM water electrolysis. Ionics 24, 3113–3121.
Shiva Kumar, S., Ramakrishna, S.U.B., Rama Devi, B., Himabindu, V., 2018d. Phosphorus-doped graphene supported palladium (Pd/PG) electrocatalyst for the hydrogen evolution reaction in PEM water electrolysis. Int. J. Green Energy 15 (10), 558–567.
Shiva Kumar, S., Ramakrishna, S.U.B., Srinivasulu Reddy, D., Bhagawan, D., Himabindu, V., 2017. Synthesis of polysulfone and zirconium oxide coated asbestos composite separators for alkaline water electrolysis. Int. J. Chem. Eng. Process Tech. 3 (1), 1035, 1-6 (2017).
Shiva Kumar, S., Ramakrishna, S.U.B., Vijaya Krishna, S., Srilatha, K., Rama Devi, B., Himabindu, V., 2018b. Synthesis of titanium (IV) oxide composite membrane for hydrogen production through alkaline water electrolysis. South Afr. J. Chem. Eng. 25, 54–61.
Siemens, ., 2021. UK, silyzer 300. https://assets.siemens-energy.com/siemens/assets/api/uuid:a193b68f-7ab4-4536-abe2-c23e01d0b526/datasheet-silyzer300.pdf (Accessed 13 August 2021).
Sunfire, ., 2021a. Hylink SOEC. Germany, https://www.sunfire.de/files/sunfire/images/content/Sunfire.de%20(neu)/Sunfire-Factsheet-HyLink-SOEC-20210303.pdf (Accessed 13 August 2021).
2021b. Sunfire-HYLINK ALKALINE. https://www.sunfire.de/files/sunfire/images/content/Sunfire.de%20(neu)/Sunfire-Factsheet-HyLink-Alkaline_20220520.pdf (Accessed 13 August 2021).
Tajuddin, A.A.H., Elumalai, G., Xi, Z., Hu, K., Jeong, S., Nagasawa, K., Fujita, J-i., Sone, Y., Ito, Y., 2021. Corrosion-resistant non-noble metal electrodes for PEM-type water electrolyzer. Int. J Hydrog. Energy 46, 38603–38611.
Thangavel, P., Kim, G., Kim, K.S., 2021. Electrochemical integration of amorphous NiFe (oxy) hydroxides on surface-activated carbon fibers for high-efficiency oxygen evolution in alkaline anion exchange membrane water electrolysis. J. Mater. Chem. A 9, 14043.
2021. TIANJIN mainland, FDQ800. http://www.cnthe.com/en/product_detail-35-43-30.html (Accessed 13 August 2021).

Tietz, F., Sebold, D., Brisse, A., Schefold, J., 2013. Degradation phenomena in a solid oxide electrolysis cell after 9000 h of operation. J. Power Sources 223, 129–135.

Upadhyay, M., Kim, A., Paramanantham, S.S.S., Kim, H., Lim, D., Lee, S., Moon, S., Lim, H.K., 2022. Three-dimensional CFD simulation of proton exchange membrane water electrolyser: performance assessment under different condition. Appl. Energy 306, 118016.

Upadhyay, M., Lee, S., Jung, S., Choi, Y., Moon, S., Lim, H.K., 2020. Systematic assessment of the anode flow field hydrodynamics in a new circular PEM water electrolyzer. Int. J. Hydrogen Energy 45, 20765–20775.

Vibhu, V., Vinke, I.C., Eichel, R-A., de, Haart.L.G.J., 2021. Cobalt substituted $Pr_2Ni_{1-x}co_xo_{4+\delta}$ (x = 0, 0.1, 0.2) oxygen electrodes: Impact on electrochemical performance and durability of solid oxide electrolysis cells. J. Power Sources 482, 228909.

Wang, J., Gao, Y., Kong, H., Kim, J., Choi, S., Ciucci, F., Hao, Y., Yang, S., Shao, Z., Lim, J., 2020a. Non-precious-metal catalysts for alkaline water electrolysis: operando characterizations, theoretical calculations, and recent advances. Chem. Soc. Rev. 49, 9154–9196.

Wang, Y., Li, W., Ma, L., Li, W., Liu, X., 2020b. Degradation of solid oxide electrolysis cells: phenomena, mechanisms, and emerging mitigation strategies—a review. J. Mater. Sci. Technol. 55, 35–55.

Wang, S., Lv, H., Tang, F., Sun, Y., Ji Zhou, W., Shen, X., Zhang, C., 2021. Defect engineering assisted support effect: IrO_2/N defective g-C_3N_4 composite as highly efficient anode catalyst in PEM water electrolysis. Chem. Eng. J. 419, 129455.

Wang, M., Wang, Z., Gong, X., Guo, Z., 2014. The intensification technologies to water electrolysis for hydrogen production—A review. Renew. Sustain. Energy Rev. 29, 573–588.

Wei, A., Siebel, A., Bernt, M., Shen, T.H., Tileli, V., Gasteiger, H.A., 2019. Impact of intermittent operation on lifetime and performance of a PEM water electrolyzer. J. Electrochem. Soc. 166, F487–F497.

Xie, Z., Yu, S., Ma, X., Li, K., Ding, L., Wang, W., Cullen, D.A., Meyer, H.M., Yu, H., Tong, J., Wu, Z., Zhang, F-Y., 2022. MoS_2 nanosheet integrated electrodes with engineered 1T-2H phases and defects for efficient hydrogen production in practical PEM electrolysis. Appl. Catal. B 313, 121458.

Xie, Z., Yu, S., Yang, G., Li, K., Ding, L., Wang, W., Cullen, D.A., Meyer, H.M., Retterer, S.T., Wu, Z., Sun, J., Gao, P-X., Zhang, F-Y., 2021. Ultrathin platinum nanowire based electrodes for high-efficiency hydrogen generation in practical electrolyzer cells. Chem. Eng. J. 410, 128333.

Xu, Z., Yeh, C-L., Chen, J-L., Lin, T.J., Ho, K-C., Lin, R.Y-Y., 2022. Metal-organic framework-derived 2D NiCoP nanoflakes from layered double hydroxide nanosheets for efficient electrocatalytic water splitting at high current densities. ACS Sustain. Chem. Eng. http://dx.doi.org/10.1021/acssuschemeng.2c03250, Published on August 23, 2022.

Yang, G., et al., 2019. A novel PEMEC with 3D printed non-conductive bipolar plate for low-cost hydrogen production from water electrolysis. Energy Convers. Manage. 182, 108–116.

Yodwong, B., Guilbert, D., Phattanasak, M., Kaewmanee, W., Hinaje, M., Vitale, G., 2020. AC-DC converters for electrolyzer applications: State of the art and future challenges. Electronics 9, 912.

Yoon, Y., Kim, H., Kim, S-K., Kim, J.J., 2021. Acid-durable, high-performance cobalt phosphide catalysts for hydrogen evolution in proton exchange membrane water electrolysis. Int. J. Energy Res. 45, 16842–16855.

Yu, F., Yu, L., Mishra, I.K., Yu, Y., Ren, Z.F., Zhou, H.Q., 2018. Recent developments in earth-abundant and non-noble electrocatalysts for water electrolysis. Mater. Today Phys. 7, 121–138.

Yue, M., Lambert, H., Pahon, E., Roche, R., Jemei, S., Hissel, D., 2021. Hydrogen energy systems: A critical review of technologies, applications, trends and challenges. Renew. Sustain. Energy Rev. 146, 111180.

Zhang, J., Fu, X., Xia, F., Zhang, W., Ma, D., Zhou, Y., Peng, H., Wu, J., Gong, X., Wang, D., Yue, Q., 2022. Core-shell nanostructured Ru@Ir–O electrocatalysts for superb oxygen evolution in acid. Small 18, 2108031.

Zhao, Z., Wang, X., Tang, S., Cheng, M., Shao, Z., 2021. High-performance oxygen electrode $Ce_{0.9}Co_{0.1}o_{2-\delta}$-LSM-YSZ for hydrogen production by solid oxide electrolysis cells. Int. J. Hydrog. Energy 46, 25332–25340.

Zheng, Y., Jiang, H., Wang, S., Qian, B., Li, Q., Ge, L., Chen, H., 2021. Mn-doped Ruddlesden-Popper oxide $La_{1.5}Sr_{0.5}NiO_{4+\delta}$ as a novel air electrode material for solid oxide electrolysis cells. Ceram. Int. 471208-471217.